

# Quantum Algorithms for Data Representation and Analysis

Armando Bellante<sup>1</sup>, Alessandro Luongo<sup>2,3</sup>, and Stefano Zanero<sup>1</sup>

<sup>1</sup>DEIB, Politecnico di Milano - Via Ponzio 34/5 – Building 20, 20133 Milan, Italy.

<sup>2</sup>IRIF, Université Paris Diderot - 8, Place Aurélie Nemours, 75205 Paris Cedex 13, France

<sup>3</sup>CQT, National University of Singapore - 3, Science Drive 2, 117543 Singapore.

We narrow the gap between previous literature on quantum linear algebra and useful data analysis on a quantum computer, providing quantum procedures that speed-up the solution of eigenproblems for data representation in machine learning. The power and practical use of these subroutines is shown through new quantum algorithms, sublinear in the input matrix’s size, for principal component analysis, correspondence analysis, and latent semantic analysis. We provide a theoretical analysis of the run-time and prove tight bounds on the randomized algorithms’ error. We run experiments on multiple datasets, simulating PCA’s dimensionality reduction for image classification with the novel routines. The results show that the run-time parameters that do not depend on the input’s size are reasonable and that the error on the computed model is small, allowing for competitive classification performances.

## 1 Introduction

Quantum computation is a computing paradigm that promises substantial speed-ups in a plethora of tasks that are computationally hard for classical computers. In 2009, a work from Harrow, Hassidim, and Lloyd [23] gave birth to the field of Quantum Machine Learning. Their work presented quantum procedures to create a quantum state proportional to the solution of a linear system of equations  $\mathbf{Ax} = \mathbf{b}$  in time logarithmic in the size of  $\mathbf{A}$ . This result has promoted further research on optimization and linear algebra problems, leading to quantum algorithms for linear regressions [8], support vector machines [49], k-means [32], and many others [3]. These algorithms achieve exponential or polynomial speed-ups over their best known classical counterparts. In this work, we focus on a critical machine learning task that can benefit from the latest quantum results: computing data representations. When handling big data, it is crucial to learn effective representations that reduce the data’s noise and help the learner perform better on the task. Many data representation methods for machine learning, such as principal component analysis [46], correspondence analysis [19], slow feature analysis [28], or latent semantic analysis [12], heavily rely on singular value decomposition and result impractical to compute on classical computers for extensive datasets.

**Our contributions** We introduce novel quantum procedures to retrieve the models of machine learning algorithms for data analysis and representation. These allow estimating

---

Armando Bellante: [armando.bellante@polimi.it](mailto:armando.bellante@polimi.it)

the most relevant singular values, factor scores, factor score ratios of an  $n \times m$  matrix in time poly-logarithmic in  $nm$ , and the most relevant singular vectors sub-linearly in  $nm$ . We show how to use these methods to estimate the models of three machine learning algorithms based on eigenvalue problems: principal component analysis, correspondence analysis, and latent semantic analysis. We also show how to represent the data in the newly computed feature space with a quantum computer. For all these algorithms and subroutines we provide a thorough theoretical analysis, giving bounds for the run-time and the error propagation of the randomized algorithms. More in general, we have gathered and combined state-of-the-art quantum techniques to present a useful and easy-to-use framework for solving eigenvalue problems at large scale. While we focus on linear problems in ML, these subroutines can be used for other problems that are classically solved via an SVD of a suitable matrix.

**Related works** The problem of singular value decomposition has been widely discussed in recent quantum computing literature [29, 31, 43, 50]. Given a quantum representation of a matrix  $\mathbf{A} = \sum_i^r \sigma_i \mathbf{u}_i \mathbf{v}_i^T$ , the results of those papers allow creating a quantum state  $|\mathbf{A}\rangle = \frac{1}{\|\mathbf{A}\|_F} \sum_i^r \sigma_i |\mathbf{u}_i\rangle |\mathbf{v}_i\rangle |\bar{\sigma}_i\rangle$ , where  $\bar{\sigma}_i$  is an estimate of  $\sigma_i$ , in time poly-logarithmic in the matrix's size. However, these works do not discuss the complexity and error of obtaining the classical singular values and vectors. To our knowledge, there are no works that provide a theoretical discussion on the extraction of the information needed by SVD based representation algorithms using quantum routines.

Other quantum algorithms that address PCA's problem are He et al. [25], Lin et al. [42], Yu et al. [62], but are either missing some steps (i.e., deciding how many singular vectors to retain) or based on old techniques, leading to slower run-times, or solving different tasks.

Following these recent quantum algorithms, there have been attempts to “de-quantize” the SVD procedures [2, 10, 54] leveraging a technique that computes a low-rank approximation of a matrix in time sub-linear in the number of its elements [14]. Even though these routines do not have explicit dependencies on the matrix's size, they generally have high polynomial dependencies on input matrix's norms and the approximation error. The most recent quantum-inspired results are the ones of Chepurko et al. [9] and Gilyén et al. [16]. In the appendix, we further discuss the de-quantizations that most challenge quantum algorithms for SVDs of low rank matrices. Similarly and independently from us, Koide-Majima and Majima [37] have extended some de-quantized subroutines to perform canonical correspondence analysis.

We refer the interested readers to the appendix, where they can find much deeper analysis on quantum and classical algorithms for eigenproblems, PCA, CA, and LSA.

## 2 Quantum preliminaries and notation

**Notation** Given a matrix  $\mathbf{A}$ , we write  $\mathbf{a}_{i\cdot}$  to denote its  $i^{th}$  row,  $\mathbf{a}_{\cdot j}$  for its  $j^{th}$  column, and  $a_{ij}$  for the element at row  $i$ , column  $j$ . We write the singular value decomposition as  $\mathbf{A} = \mathbf{U}\Sigma\mathbf{V}^T$ .  $\mathbf{U}$  and  $\mathbf{V}$  are orthogonal matrices, whose column vectors,  $\mathbf{u}_i$  and  $\mathbf{v}_i$ , are respectively the left and right singular vectors of  $\mathbf{A}$ .  $\Sigma$  is a diagonal matrix with positive, non-zero, elements  $\sigma_i$ : the singular values of  $\mathbf{A}$ . The row/column size of  $\Sigma$  is the rank of  $\mathbf{A}$  and is denoted as  $r$ . We use:  $\lambda_i$  to denote the  $i^{th}$  eigenvalue of the covariance matrix  $\mathbf{A}^T\mathbf{A} = \mathbf{V}\Sigma^2\mathbf{V}^T$ ;  $\lambda^{(i)} = \frac{\lambda_i}{\sum_j^r \lambda_j}$  to denote the relative magnitude of each eigenvalue. Using the notation of Hsu et al. [26] for correspondence analysis, we refer to  $\lambda_i$  as factor scores and to  $\lambda^{(i)}$  as factor score ratios. Note that  $\lambda_i = \sigma_i^2$  and  $\lambda^{(i)} = \frac{\sigma_i^2}{\sum_j^r \sigma_j^2}$ .

We denote the number of non-zero elements of a matrix/vector with  $nnz()$ . The  $\ell_p$  norm of a vector  $\mathbf{a} \in \mathbb{R}^n$  is  $\|\mathbf{a}\|_p = (\sum_i^n |a_i|^p)^{1/p}$ . When  $p$  is not specified we mean the  $\ell_2$  norm. There are two exceptions:  $\|\mathbf{a}\|_\infty = \max_i(|a_i|)$ ,  $\|\mathbf{a}\|_0 = nnz(\mathbf{a})$ . For what concern matrices: the Frobenius norm is  $\|\mathbf{A}\|_F = \sqrt{\sum_i^r \sigma_i^2}$ , the spectral norm is  $\|\mathbf{A}\| = \max_{\mathbf{x} \in \mathbb{R}^m} \frac{\|\mathbf{Ax}\|}{\|\mathbf{x}\|} = \sigma_{max}$ , and  $\|\mathbf{A}\|_\infty = \max_i(\|\mathbf{a}_{i,\cdot}\|_1)$ . Given a scalar  $a$ ,  $\|a\|$  is its absolute value. Given a complex number  $\alpha$ ,  $|\alpha|$  is its module.

A contingency table is a matrix that represents categorical variables in terms of the observed frequency counts. Finally, when stating the complexity of an algorithm, we use  $\tilde{O}$  instead of  $O$  to omit the poly-logarithmic terms on the size of the input data, so  $O(\text{polylog}(nm)) = \tilde{O}(1)$ .

**Processing framework** We represent scalars as states of the computational basis of  $\mathcal{H}_n$ , where  $n$  is the number of bits required for binary encoding. The quantum state corresponding to a vector  $\mathbf{v} \in \mathbb{R}^m$  is defined as a *state-vector*  $|\mathbf{v}\rangle = \frac{1}{\|\mathbf{v}\|} \sum_j^m v_j |j\rangle$ . Note that to build  $|\mathbf{v}\rangle$  we need  $\lceil \log m \rceil$  qubits. To access data in the form of state-vectors, we use the following definition of efficient quantum access.

**Definition 1** (Efficient quantum access). *We have efficient quantum access to a matrix  $\mathbf{A} \in \mathbb{R}^{n \times m}$ , if there exists a data structure that allows performing the mappings  $|i\rangle |0\rangle \mapsto |i\rangle |\mathbf{a}_{i,\cdot}\rangle = |i\rangle \frac{1}{\|\mathbf{a}_{i,\cdot}\|} \sum_j^m a_{ij} |j\rangle$ , for all  $i$ , and  $|0\rangle \mapsto \frac{1}{\|\mathbf{A}\|_F} \sum_i^n \|\mathbf{a}_{i,\cdot}\| |i\rangle$  in time  $\tilde{O}(1)$ .*

By combining the two oracles we can create the state  $|\mathbf{A}\rangle = \frac{1}{\|\mathbf{A}\|_F} \sum_i^n \sum_j^m a_{ij} |i\rangle |j\rangle$  in time  $\tilde{O}(1)$ . One implementation of such efficient quantum data access has been described in Kerenidis and Luongo [28], Kerenidis and Prakash [29, 31]. Their implementation is based on a classical data structure such that the cost of updating/deleting/inserting one element of the matrix is poly-logarithmic in the number of its components. In addition, their structure gives access to the Frobenius norm of the matrix and the norm of its rows in time  $O(1)$ . The cost of creating this data structure is  $\tilde{O}(nnz(\mathbf{A}))$ .

Throughout the work, we require that matrices are normalized so that their greatest singular value is smaller than one. Kerenidis and Prakash [31], provide an efficient pre-processing for this normalization.

**Theorem 2** (Spectral norm estimation [31]). *Let there be efficient quantum access to the matrix  $\mathbf{A} \in \mathbb{R}^{n \times m}$ , and let  $\epsilon > 0$  be a precision parameter. There exists a quantum algorithm that estimates  $\|\mathbf{A}\|$  to error  $\epsilon \|\mathbf{A}\|_F$  in time  $\tilde{O}\left(\frac{\log(1/\epsilon)}{\epsilon} \frac{\|\mathbf{A}\|_F}{\|\mathbf{A}\|}\right)$ .*

The normalization algorithm consists in using Theorem 2 to estimate  $\|\mathbf{A}\|$  and creating access to  $\mathbf{A}' = \frac{\mathbf{A}}{\|\mathbf{A}\|} = \mathbf{U} \frac{\boldsymbol{\Sigma}}{\sigma_{max}} \mathbf{V}^T$ . Since all the entries in  $\boldsymbol{\Sigma}$  are  $0 < \sigma_i \leq \sigma_{max}$ , we have that the singular values of  $\mathbf{A}'$  are normalized between 0 and 1, while the left and right singular vectors remain the same. The cost of preparing efficient quantum access to the normalized matrix  $\mathbf{A}'$  is  $\tilde{O}(nnz(\mathbf{A}))$ . Once a dataset is stored in an adequate data structure that satisfies Definition 1 (e.g. KP-Trees), it is possible to apply a pipeline of quantum machine learning algorithms for data representation, analysis, clustering, and classification [1, 28, 32, 36, 48, 55]. Since the cost of each step of the pipeline should be evaluated independently from the one of storing the data, which is a necessary cost in any case, we consider  $\tilde{O}(nnz(\mathbf{A}))$  as a pre-processing cost (which can be performed when the data is received) and we do not include it in the run-times of our algorithms.

We state two relevant quantum linear algebra results: quantum singular value estimation (SVE) and quantum matrix-vector multiplication.

**Theorem 3** (Singular value estimation [31]). *Let there be efficient quantum access to  $\mathbf{A} \in \mathbb{R}^{n \times m}$ , with singular value decomposition  $\mathbf{A} = \sum_i^r \sigma_i \mathbf{u}_i \mathbf{v}_i^T$  and  $r = \min(n, m)$ . Let  $\epsilon > 0$  be a precision parameter. It is possible to perform the mapping  $|b\rangle = \sum_i \alpha_i |\mathbf{v}_i\rangle \mapsto \sum_i \alpha_i |\mathbf{v}_i\rangle |\bar{\sigma}_i\rangle$ , such that  $\|\sigma_i - \bar{\sigma}_i\| \leq \epsilon$  with probability at least  $1 - 1/\text{poly}(m)$ , in time  $\tilde{O}(\frac{\mu(\mathbf{A})}{\epsilon})$  where  $\mu(\mathbf{A}) = \min_{p \in [0,1]} (\|\mathbf{A}\|_F, \sqrt{s_{2p}(\mathbf{A})s_{2(p-1)}(\mathbf{A}^T)})$  and  $s_p(\mathbf{A}) = \max_i \|\mathbf{a}_i, \cdot\|_p^p$ .*

This algorithm allows us to perform conditional rotations using the singular values of a matrix without any special requirement on its properties (e.g., sparsity, being Hermitian, etc.). By choosing the same matrix  $|\mathbf{A}\rangle = \frac{1}{\|\mathbf{A}\|_F} \sum_i^k \sigma_i |\mathbf{u}_i\rangle |\mathbf{v}_i\rangle$  as starting state  $|b\rangle$ , we can drop the requirement on the rank. It is important to remark that this algorithm uses consistent phase estimation, so that the errors in the estimates of the singular values are consistent across multiple runs [31].

**Theorem 4** (Matrix-vector multiplication [8] (Lemma 24)). *Let there be efficient quantum access to the matrix  $\mathbf{A} \in \mathbb{R}^{n \times n}$ , with  $\sigma_{\max} \leq 1$ , and to a vector  $\mathbf{x} \in \mathbb{R}^n$ . Let  $\|\mathbf{A}\mathbf{x}\| \geq \gamma$ . There exists a quantum algorithm that creates a state  $|\mathbf{z}\rangle$  such that  $\|\mathbf{z}\rangle - |\mathbf{A}\mathbf{x}\rangle\| \leq \epsilon$  in time  $\tilde{O}(\frac{1}{\gamma} \mu(\mathbf{A}) \log(1/\epsilon))$ , with probability at least  $1 - 1/\text{poly}(n)$ . Increasing the run-time by a multiplicative factor  $\tilde{O}(\frac{1}{\eta})$  one can retrieve an estimate of  $\|\mathbf{A}\mathbf{x}\|$  to relative error  $\eta$ .*

This result stems from the recent techniques of block-encodings and qubitization [8, 15, 44], which provide many fast linear algebra operations on matrices and vectors.

Finally, we state one version of amplitude amplification and estimation, and two *state-vector* tomographies.

**Theorem 5** (Amplitude amplification and estimation [4, 34]). *Given a unitary that performs the mapping  $U_x : |0\rangle \mapsto \sin(\theta) |\mathbf{x}, 0\rangle + \cos(\theta) |\mathbf{G}, 0^\perp\rangle$  in time  $T(U_x)$ , then  $\sin(\theta)^2$  can be estimated to multiplicative error  $\eta$  in time  $O(\frac{T(U_x)}{\eta \sin(\theta)})$  and  $|\mathbf{x}\rangle$  can be generated in expected time  $O(\frac{T(U_x)}{\sin(\theta)})$ .*

**Theorem 6** ( $\ell_2$  state-vector tomography [30, 34]). *Given a unitary mapping  $U_x : |0\rangle \mapsto |\mathbf{x}\rangle$  in time  $T(U_x)$  and  $\delta > 0$ , there is an algorithm that produces an estimate  $\bar{\mathbf{x}} \in \mathbb{R}^m$  with  $\|\bar{\mathbf{x}}\| = 1$  such that  $\|\mathbf{x} - \bar{\mathbf{x}}\| \leq \delta$  with probability at least  $1 - 1/\text{poly}(m)$  in time  $O(T(U_x) \frac{m \log m}{\delta^2})$ .*

**Theorem 7** ( $\ell_\infty$  state-vector tomography [33]). *Given access to a unitary mapping  $U_x : |0\rangle \mapsto |\mathbf{x}\rangle$  and its controlled version in time  $T(U_x)$ , and  $\delta > 0$ , there is an algorithm that produces an estimate  $\bar{\mathbf{x}} \in \mathbb{R}^m$  with  $\|\bar{\mathbf{x}}\| = 1$  such that  $\|\mathbf{x} - \bar{\mathbf{x}}\|_\infty \leq \delta$  with probability at least  $1 - 1/\text{poly}(m)$  in time  $O(T(U_x) \frac{\log m}{\delta^2})$ .*

### 3 Novel quantum methods

Building from the previous section’s techniques, we formalize a series of quantum algorithms that allow us to retrieve a classical description of the singular value decomposition of a matrix to which we have efficient quantum access. In particular, we formalize a procedure to estimate the most relevant singular values, factor scores, and factor score ratios of a matrix in time that is poly-logarithmic in the number of its components, and a procedure to extract the most relevant singular vectors in time that is sub-linear in the matrix’s size. Proofs of the statements can be found in the appendix.

### 3.1 Estimating the quality of the representation

Algorithms such as principal component analysis and correspondence analysis are often used for data visualization or dimensionality reduction purposes. These applications work better when there is a subset of factor scores with a significant factor score ratio. We provide a fast procedure that allows verifying if this is the case: given efficient quantum access to a matrix  $\mathbf{A} \in \mathbb{R}^{n \times m}$ , it retrieves the most relevant singular values, factor scores, and factor score ratios in time poly-logarithmic in the number of elements of  $\mathbf{A}$ , with no strict dependencies on its rank.

The main intuition behind this algorithm is that it is possible to create the state  $\sum_i^r \sqrt{\lambda^{(i)}} |\mathbf{u}_i\rangle |\mathbf{v}_i\rangle |\bar{\sigma}_i\rangle$  and that the third register, when measured in the computational basis, outputs the estimate  $\bar{\sigma}_i$  of a singular value with probability equal to its factor score ratio  $\lambda^{(i)}$ . This allows us to sample the singular values of  $\mathbf{A}$  directly from the factor score ratios' distribution. When a matrix has a huge number of small singular values and only a few of them that are very big, the ones with the greatest factor score ratios will appear many times during the measurements, while the negligible ones are not likely to be measured. This intuition has already appeared in literature [6, 21]. Nevertheless, the analysis and the problem solved are different, making the run-time analysis unrelated. This idea in the context of data representation and analysis, this intuition has only been sketched for sparse or low rank square symmetric matrices, by Lloyd et al. [43], without a precise formalization. We thoroughly formalize it, in a data representation and analysis context, for any real matrix.

---

**Algorithm 1** Quantum factor score ratio estimation.

---

```

1:  $S = 0$ 
2: while  $S < \tilde{O}\left(\frac{1}{\gamma^2}\right)$  do
3:   Prepare the state  $\frac{1}{\|\mathbf{A}\|_F} \sum_i^n \sum_j^m a_{ij} |i\rangle |j\rangle$ .
4:   Apply SVE to get  $\frac{1}{\sqrt{\sum_j^r \sigma_j^2}} \sum_i^r \sigma_i |\mathbf{u}_i\rangle |\mathbf{v}_i\rangle |\bar{\sigma}_i\rangle$ .
5:   Measure the last register and store a counter of how many times each distinct value
    $|\bar{\sigma}_i\rangle$  is measured.
6:    $S = S + 1$ 
7: end while
8: For each distinct  $\bar{\sigma}_i$  measured, output  $\bar{\sigma}_i$  and its factor score  $\bar{\lambda}_i = \bar{\sigma}_i^2$ .
9: For each distinct  $\bar{\sigma}_i$  measured, output its factor score ratio  $\bar{\lambda}^{(i)} = \frac{\zeta_{\bar{\sigma}_i}}{S}$ , where  $\zeta_{\bar{\sigma}_i}$  is
   the number of times  $|\bar{\sigma}_i\rangle$  has been observed among the measurements. Each estimate
   comes with confidence level  $z$ .

```

---

**Theorem 8** (Quantum factor score ratio estimation). *Let there be efficient quantum access to a matrix  $\mathbf{A} \in \mathbb{R}^{n \times m}$ , with singular value decomposition  $\mathbf{A} = \sum_i \sigma_i \mathbf{u}_i \mathbf{v}_i^T$  and  $\sigma_{\max} \leq 1$ . Let  $\gamma, \epsilon$  be precision parameters. There exists a quantum algorithm that, in time  $\tilde{O}\left(\frac{1}{\gamma^2} \frac{\mu(\mathbf{A})}{\epsilon}\right)$ , estimates:*

- the factor score ratios  $\lambda^{(i)}$ , such that  $\|\lambda^{(i)} - \bar{\lambda}^{(i)}\| \leq \gamma$ , with high probability;
- the correspondent singular values  $\sigma_i$ , such that  $\|\sigma_i - \bar{\sigma}_i\| \leq \epsilon$ , with probability at least  $1 - 1/\text{poly}(n)$ ;
- the correspondent factor scores  $\lambda_i$ , such that  $\|\lambda_i - \bar{\lambda}_i\| \leq 2\epsilon$ , with probability at least  $1 - 1/\text{poly}(n)$ .

The parameter  $\gamma$  is the one that controls how big a factor score ratio should be for

the singular value/factor score to be measured. If we choose  $\gamma$  bigger than the least factor scores ratio of interest, the estimate for the smaller ones is likely to be 0, as  $\|\lambda^{(i)} - 0\| \leq \gamma$  would be a plausible estimation.

Often in data representations, the cumulative sum of the factor score ratios is a measure of the quality of the representation. By slightly modifying Algorithm 1 to use Theorem 7, it is possible to estimate this sum such that  $\|\sum_i^k \lambda^{(i)} - \sum_i^k \bar{\lambda}^{(i)}\| \leq k\epsilon$  with probability  $1 - 1/\text{poly}(r)$ . However, a slight variation of the algorithm of Theorem 2 provides a more accurate estimation in less time, given a threshold  $\theta$  for the smallest singular value to retain.

**Theorem 9** (Quantum check on the factor score ratios' sum). *Let there be efficient quantum access to the matrix  $\mathbf{A} \in \mathbb{R}^{n \times m}$ , with singular value decomposition  $\mathbf{A} = \sum_i \sigma_i \mathbf{u}_i \mathbf{v}_i^T$ . Let  $\eta, \epsilon$  be precision parameters and  $\theta$  be a threshold for the smallest singular value to consider. There exists a quantum algorithm that estimates  $p = \frac{\sum_{i: \bar{\sigma}_i \geq \theta} \sigma_i^2}{\sum_j \sigma_j^2}$ , where  $\|\sigma_i - \bar{\sigma}_i\| \leq \epsilon$ , to relative error  $\eta$  in time  $\tilde{O}\left(\frac{\mu(\mathbf{A})}{\epsilon} \frac{1}{\eta \sqrt{p}}\right)$ .*

Moreover, we borrow an observation from Kerenidis and Prakash [31] on Theorem 2, to perform a binary search of  $\theta$  given the desired sum of factor score ratios.

**Theorem 10** (Quantum binary search for the singular value threshold [31]). *Let there be efficient quantum access to the matrix  $\mathbf{A} \in \mathbb{R}^{n \times m}$ . Let  $p$  be the factor ratios sum to retain. The threshold  $\theta$  for the smallest singular value to retain can be estimated to absolute error  $\epsilon$  in time  $\tilde{O}\left(\frac{\log(1/\epsilon)\mu(\mathbf{A})}{\epsilon \sqrt{p}}\right)$ .*

Both these procedures are very fast. In problems such as PCA, CA, and LSA, the desired sum of factor score ratios to retain is a number in the range  $p \in [1/3, 1]$  with precision up to the second decimal digit. In practice, the complexity of these last two algorithms scales as  $\tilde{O}\left(\frac{\mu(\mathbf{A})}{\epsilon}\right)$ .

### 3.2 Extracting the SVD representation

After introducing the procedures to test for the most relevant singular values, factor scores and factor score ratios of  $\mathbf{A}$ , we present an efficient routine to extract the corresponding right/left singular vectors. The inputs of this algorithm, other than the matrix, are a parameter  $\delta$  for the precision of the singular vectors, a parameter  $\epsilon$  for the precision of the singular value estimation, and a threshold  $\theta$  to discard the non interesting singular values/vectors. The output guarantees a unit estimate  $\bar{\mathbf{x}}_i$  of each singular vector such that  $\|\mathbf{x}_i - \bar{\mathbf{x}}_i\|_\ell \leq \delta$  for  $\ell \in \{2, \infty\}$ , ensuring that the estimate has a similar orientation to the original vector. Additionally, this subroutine can provide an estimation of the singular values greater than  $\theta$ , to absolute error  $\epsilon$ .

---

**Algorithm 2** Quantum top-k singular vectors extraction.

---

- 1: Prepare the state  $\frac{1}{\|\mathbf{A}\|_F} \sum_i^n \sum_j^m a_{ij} |i\rangle |j\rangle$ .
- 2: Apply SVE to get  $\frac{1}{\sqrt{\sum_j^r \sigma_j^2}} \sum_i^r \sigma_i |\mathbf{u}_i\rangle |\mathbf{v}_i\rangle |\bar{\sigma}_i\rangle$ .
- 3: Append a quantum register  $|0\rangle$  to the state and set it to  $|1\rangle$  if  $|\bar{\sigma}_i\rangle < \theta$ .
- 4: Perform amplitude amplification for  $|0\rangle$ , to get the state  $\frac{1}{\sqrt{\sum_j^k \sigma_j^2}} \sum_i^k \sigma_i |\mathbf{u}_i\rangle |\mathbf{v}_i\rangle |\bar{\sigma}\rangle$ .
- 5: Append a second ancillary register  $|0\rangle$  and perform the controlled rotation  $\frac{C}{\|\mathbf{A}^{(k)}\|_F} \sum_i^k \frac{\sigma_i}{\bar{\sigma}_i} |\mathbf{u}_i\rangle |\mathbf{v}_i\rangle |\bar{\sigma}_i\rangle |0\rangle + \frac{1}{\|\mathbf{A}^{(k)}\|_F} \sum_i^k \sqrt{1 - \frac{C^2}{\bar{\sigma}_i^2}} |\mathbf{u}_i\rangle |\mathbf{v}_i\rangle |\bar{\sigma}_i\rangle |1\rangle$  where  $C$  is a normalization constant.
- 6: Perform again amplitude amplification for  $|0\rangle$  to get  $\frac{1}{\sqrt{k}} \sum_i^k |\mathbf{u}_i\rangle |\mathbf{v}_i\rangle |\bar{\sigma}_i\rangle$ .
- 7: Measure the last register and, according to the measured  $|\bar{\sigma}_i\rangle$ , apply state-vector tomography on  $|\mathbf{u}_i\rangle$  for the  $i^{th}$  left singular vector or on  $|\mathbf{v}_i\rangle$  for the right one.
- 8: Repeat 1-7 until the tomography requirements are met.
- 9: Output the  $k$  singular vectors  $\mathbf{u}_i$  or  $\mathbf{v}_i$  and, optionally, the singular values  $\bar{\sigma}_i$ .

---

**Theorem 11** (Top-k singular vectors extraction). *Let there be efficient quantum access to the matrix  $\mathbf{A} \in \mathbb{R}^{n \times m}$ , with singular value decomposition  $\mathbf{A} = \sum_i^r \sigma_i \mathbf{u}_i \mathbf{v}_i^T$  and  $\sigma_{\max} \leq 1$ . Let  $\delta > 0$  be a precision parameter for the singular vectors,  $\epsilon > 0$  a precision parameter for the singular values, and  $\theta > 0$  be a threshold such that  $\mathbf{A}$  has  $k$  singular values greater than  $\theta$ . Define  $p = \frac{\sum_{i: \bar{\sigma}_i \geq \theta} \sigma_i^2}{\sum_j \sigma_j^2}$ . There exist quantum algorithms that estimate:*

- The top  $k$  left singular vectors  $\mathbf{u}_i$  of  $\mathbf{A}$  with unit vectors  $\bar{\mathbf{u}}_i$  such that  $\|\mathbf{u}_i - \bar{\mathbf{u}}_i\|_2 \leq \delta$  with probability at least  $1 - 1/\text{poly}(n)$ , in time  $\tilde{O}\left(\frac{1}{\theta} \frac{1}{\sqrt{p}} \frac{\mu(\mathbf{A})}{\epsilon} \frac{kn}{\delta^2}\right)$ ;
- The top  $k$  right singular vectors  $\mathbf{v}_i$  of  $\mathbf{A}$  with unit vectors  $\bar{\mathbf{v}}_i$  such that  $\|\mathbf{v}_i - \bar{\mathbf{v}}_i\|_2 \leq \delta$  with probability at least  $1 - 1/\text{poly}(m)$ , in time  $\tilde{O}\left(\frac{1}{\theta} \frac{1}{\sqrt{p}} \frac{\mu(\mathbf{A})}{\epsilon} \frac{km}{\delta^2}\right)$ .
- The top  $k$  singular values  $\sigma_i$  and factor scores  $\lambda_i$  of  $\mathbf{A}$  to precision  $\epsilon$  and  $2\epsilon$  with probability at least  $1 - 1/\text{poly}(m)$ , in time  $\tilde{O}\left(\frac{1}{\theta} \frac{1}{\sqrt{p}} \frac{\mu(\mathbf{A})k}{\epsilon}\right)$  or any of the two above.

Besides  $p$  being negligible, it is interesting to note that the parameter  $\theta$  can be computed using: 1. the procedures of Theorems 8 and 9; 2. the binary search of Theorem 10; 3. the available literature on the type of data stored in the input matrix  $\mathbf{A}$ . About the latter, the original paper of latent semantic indexing [12] states that the first  $k = 100$  singular values are enough for a good representation. We believe that, in the same way, fixed thresholds  $\theta$  can be defined for different machine learning applications. The experiments of Kerenidis and Luongo [28] on the run-time parameters of the polynomial expansions of the MNIST dataset support this expectation: even though in qSFA they keep the  $k$  smallest singular values and refer to  $\theta$  as the biggest singular value to retain, this value does not vary much when the the dimensionality of their dataset grows. In our experiments, we observe that different datasets for image classification have similar  $\theta$ s.

We also state a different version of Theorem 11, with  $\ell_\infty$  guarantees on the vectors.

**Corollary 12** (Fast top-k singular vectors extraction). *The run-times of 11 can be improved to  $\tilde{O}\left(\frac{1}{\theta} \frac{1}{\sqrt{p}} \frac{\mu(\mathbf{A})}{\epsilon} \frac{k}{\delta^2}\right)$  with estimation guarantees on the  $\ell_\infty$  norms.*

Note that, given a vector with  $d$  non-zero entries, performing  $\ell_\infty$  tomography with error  $\frac{\delta}{\sqrt{d}}$  provides the same guarantees of  $\ell_2$  tomography with error  $\delta$ . In practice, this result implies that the extraction of the singular vectors, with  $\ell_2$  guarantees, can be faster if we can assume some prior assumptions on their sparseness:  $\tilde{O}\left(\frac{1}{\theta} \frac{1}{\sqrt{p}} \frac{\mu(\mathbf{A})}{\epsilon} \frac{kd}{\delta^2}\right)$ .

## 4 Applications to machine learning

We show how to use the novel quantum procedures to extract the models of principal component analysis, correspondence analysis, and latent semantic analysis, discussing the run-time and the errors on the models. We provide a procedure to represent the new data on a quantum device in case of PCA’s dimensionality reduction, in a similar way it is possible to derive the representation of CA and LSA. Formal proofs of our statements can be found in the appendix, together with further discussion on the corollaries.

### 4.1 Principal Component Analysis

Principal component analysis is a widely-used multivariate statistical method for continuous variables that finds many applications in machine learning, ranging from outlier detection to dimensionality reduction and data visualization. Given a matrix  $\mathbf{A} \in \mathbb{R}^{n \times m}$  that stores information about  $n$  data points using  $m$  coordinates, its *principal components* are the set of orthogonal vectors along which the variance of the data points is maximized. The goal of PCA is to compute the principal components, with the amount of variance they capture, and rotate the data-points to make the axis coincide with the principal components. For dimensionality reduction, it is possible to represent the data using only the  $k$  coordinates that express most variance.

**Model** The model of PCA is closely related to the singular value decomposition of the data matrix  $\mathbf{A}$ , shifted to row mean 0. The principal components coincide with the right singular vectors  $\mathbf{v}_i$ . The factor scores  $\lambda_i = \sigma_i^2$  represent the amount of variance along each of them and the factor score ratios  $\lambda^{(i)} = \frac{\lambda_i}{\sum_j \lambda_j}$  express the percentage of the variance retained. For datasets with 0 mean, the transformation consists in a rotation along the principal components:  $\mathbf{Y} = \mathbf{AV} = \mathbf{U}\Sigma\mathbf{V}^T\mathbf{V} = \mathbf{U}\Sigma \in \mathbb{R}^{n \times m}$ . Therefore, the data points in the new subspace can be computed using the left singular vectors and the singular values of  $\mathbf{A}$ . When performing dimensionality reduction it suffice to use only the top  $k$  singular values and vectors.

Using the procedures from Section 3 it is possible to extract the model for principal component analysis. Theorems 8, 9 allow to retrieve information on the factor scores and on the factor score ratios, while Theorem 11 allows extracting the principal components. The run-time of the model extraction is the sum of the run-times of the theorems:  $\tilde{O}\left(\left(\frac{1}{\gamma^2} + \frac{km}{\theta\delta^2}\right) \frac{\mu(\mathbf{A})}{\epsilon}\right)$ . The model comes with the following guarantees:  $\|\sigma_i - \bar{\sigma}_i\| \leq \frac{\epsilon}{2}$ ;  $\|\lambda_i - \bar{\lambda}_i\| \leq \epsilon$ ;  $\|\lambda^{(i)} - \bar{\lambda}^{(i)}\| \leq \gamma$ ;  $\|\mathbf{v}_i - \bar{\mathbf{v}}_i\| \leq \delta$  for  $i \in \{0, k-1\}$ . This run-time is generally smaller than the number of elements of the input data matrix, providing polynomial speed-ups on the best classical routines for non-sparse matrices. In writing the time complexity of the routines, we have omitted the term  $\frac{1}{\sqrt{p}}$  because usually  $p$  is chosen to be a number greater than 0.5 (generally in the order of 0.8/0.9).

When performing dimensionality reduction, the goal is to obtain the matrix  $\mathbf{Y} = \mathbf{U}\Sigma \in \mathbb{R}^{n \times k}$ , where  $\mathbf{U} \in \mathbb{R}^{n \times k}$  and  $\Sigma \in \mathbb{R}^{k \times k}$  are composed respectively by the top  $k$  left singular vectors and singular values. When this is the case, the user might want to extract the top  $k$   $\mathbf{u}_i$  and  $\sigma_i$  rather than the principal components, to avoid matrix multiplication. In Lemma 13, we provide a theoretical error bound for  $\mathbf{Y}$ , using the estimated entries of  $\mathbf{U}$  and  $\Sigma$ . For sake of completeness, the error bound is also stated for  $\mathbf{V}\Sigma$ .

**Lemma 13** (Accuracy of  $\bar{\mathbf{U}}\bar{\Sigma}$  and  $\bar{\mathbf{V}}\bar{\Sigma}$ ). *Let  $\mathbf{A} \in \mathbb{R}^{n \times m}$  be a matrix with  $\sigma_{\max} \leq 1$ . Given some approximate procedures to retrieve estimates  $\bar{\sigma}_i$  of the singular values  $\sigma_i$  such that  $\|\sigma_i - \bar{\sigma}_i\| \leq \epsilon$  and unit estimates  $\bar{\mathbf{u}}_i$  of the left singular vectors  $\mathbf{u}_i$  such that  $\|\bar{\mathbf{u}}_i - \mathbf{u}_i\|_2 \leq \delta$ , the error on  $\bar{\mathbf{U}}\bar{\Sigma}$  can be bounded as  $\|\mathbf{U}\Sigma - \bar{\mathbf{U}}\bar{\Sigma}\|_F \leq \sqrt{k}(\epsilon + \delta)$ . Similarly,  $\|\mathbf{V}\Sigma - \bar{\mathbf{V}}\bar{\Sigma}\|_F \leq \sqrt{k}(\epsilon + \delta)$ .*

The fact that the matrix has been normalized to have a spectral norm smaller than one is usually not relevant for the final applications of PCA. However, if one desires to represent transformation of the not-normalized matrix  $\mathbf{A}$ , the error bounds become the ones of Claim 14.

**Claim 14** (Non-normalized  $\bar{\mathbf{U}}\bar{\Sigma}$  and  $\bar{\mathbf{V}}\bar{\Sigma}$ ). *The estimated representations of Lemma 13, for the not-normalized matrix  $\mathbf{A}$ , are  $\|\mathbf{A}\|\bar{\mathbf{U}}\bar{\Sigma}$  and  $\|\mathbf{A}\|\bar{\mathbf{V}}\bar{\Sigma}$ . The error bounds become  $\|\|\mathbf{A}\|\mathbf{U}\Sigma - \|\mathbf{A}\|\bar{\mathbf{U}}\bar{\Sigma}\|_F \leq \sqrt{k}\|\mathbf{A}\|(\epsilon + \delta)$  and  $\|\|\mathbf{A}\|\mathbf{V}\Sigma - \|\mathbf{A}\|\bar{\mathbf{V}}\bar{\Sigma}\|_F \leq \sqrt{k}\|\mathbf{A}\|(\epsilon + \delta)$*

Based on Theorem 4, we also provide algorithms to produce quantum states proportional to the data representation in the new feature space. After  $\mathbf{V}^{(k)} \in \mathbb{R}^{m \times k}$  has been extracted, these routines create the new data points in almost constant time and are therefore useful when these states are used in a deep quantum machine learning pipeline.

**Corollary 15** (Quantum PCA: vector dimensionality reduction). *Let  $\xi$  be a precision parameter. Let there be efficient quantum access to the top  $k$  right singular vectors  $\bar{\mathbf{V}}^{(k)} \in \mathbb{R}^{m \times k}$  of a matrix  $\mathbf{A} = \mathbf{U}\Sigma\mathbf{V}^T \in \mathbb{R}^{n \times m}$ , such that  $\|\mathbf{V}^{(k)} - \bar{\mathbf{V}}^{(k)}\| \leq \frac{\xi}{\sqrt{2}}$ . Given efficient quantum access to a row  $\mathbf{a}_i$  of  $\mathbf{A}$ , the quantum state  $|\bar{\mathbf{y}}_i\rangle = \frac{1}{\|\bar{\mathbf{y}}_i\|} \sum_i^k \bar{y}_k |i\rangle$ , proportional to its projection onto the PCA space, can be created in time  $\tilde{O}\left(\frac{\|\mathbf{a}_i\|}{\|\bar{\mathbf{y}}_i\|}\right)$  with probability at least  $1 - 1/\text{poly}(m)$  and precision  $\|\mathbf{y}_i - \bar{\mathbf{y}}_i\| \leq \frac{\|\mathbf{a}_i\|}{\|\bar{\mathbf{y}}_i\|} \xi$ . An estimate of  $\|\bar{\mathbf{y}}_i\|$ , to relative error  $\eta$ , can be computed in  $\tilde{O}(1/\eta)$ .*

This result also holds when  $\mathbf{a}_i$  is a new data point, not necessarily stored in  $\mathbf{A}$ . Note that  $\frac{\|\mathbf{y}_i\|}{\|\mathbf{a}_i\|}$  is expected to be close to 1, as it is the percentage of support of  $\mathbf{a}_i$  on the new feature space spanned by  $\mathbf{V}^{(k)}$ . We formalize this better using Definition 18 below.

**Corollary 16** (Quantum PCA: matrix dimensionality reduction). *Let  $\xi$  be a precision parameter and  $p$  be the amount of variance retained after the dimensionality reduction. Let there be efficient quantum access to  $\mathbf{A} = \mathbf{U}\Sigma\mathbf{V}^T \in \mathbb{R}^{n \times m}$  and to its top  $k$  right singular vectors  $\bar{\mathbf{V}}^{(k)} \in \mathbb{R}^{m \times k}$ , such that  $\|\mathbf{V}^{(k)} - \bar{\mathbf{V}}^{(k)}\| \leq \frac{\xi\sqrt{p}}{\sqrt{2}}$ . There exists a quantum algorithm that, with probability at least  $1 - 1/\text{poly}(m)$ , creates the state  $|\bar{\mathbf{Y}}\rangle = \frac{1}{\|\bar{\mathbf{Y}}\|_F} \sum_i^n \|\mathbf{y}_i\| |i\rangle |\mathbf{y}_i\rangle$ , proportional to the projection of  $\mathbf{A}$  in the PCA subspace, with error  $\|\mathbf{Y} - |\bar{\mathbf{Y}}\rangle\| \leq \xi$  in time  $\tilde{O}(1/\sqrt{p})$ . An estimate of  $\|\bar{\mathbf{Y}}\|_F$ , to relative error  $\eta$ , can be computed in  $\tilde{O}(\frac{1}{\sqrt{p}\eta})$ .*

The error requirements of the two corollary propagate to the run-time of the model extraction in the following way.

**Corollary 17** (Quantum PCA: fitting time). *Let  $\epsilon$  be a precision parameter and  $p = \frac{\sum_{i: \bar{\sigma}_i \geq \theta} \sigma_i^2}{\sum_j \sigma_j^2}$  the amount of variance to retain, where  $\|\sigma_i - \bar{\sigma}_i\| \leq \epsilon$ . Given efficient quantum access to a matrix  $\mathbf{A} \in \mathbb{R}^{n \times m}$ , the run-time to extract  $\mathbf{V}^{(k)} \in \mathbb{R}^{m \times k}$  for corollaries 15, 16 is  $\tilde{O}\left(\frac{\mu(\mathbf{A})k^2m}{\theta\epsilon\xi^2}\right)$ .*

If the algorithm is training the model for Corollary 16, the run-time has a dependency on  $1/p^{3/2}$ , but this term is constant and independent from the size of the input dataset. With this additional  $1/p^{3/2}$  cost, the error of Corollary 15 drops to  $\xi$  for every row of the matrix and generally decreases in case of new data points.

**Definition 18** (PCA-representable data). *A set of  $n$  data points described by  $m$  coordinates, represented through a matrix  $\mathbf{A} = \sum_i^r \sigma_i \mathbf{u}_i \mathbf{v}_i^T \in \mathbb{R}^{n \times m}$  is said to be PCA-representable if there exists  $p \in [\frac{1}{2}, 1], \varepsilon \in [0, 1/2], \beta \in [p - \varepsilon, p + \varepsilon], \alpha \in [0, 1]$  such that:*

- $\exists k \in O(1)$  such that  $\frac{\sum_i^k \sigma_i^2}{\sum_i^m \sigma_i^2} = p$
- for at least  $\alpha n$  points  $\mathbf{a}_i$  it holds  $\frac{\|\mathbf{y}_i\|}{\|\mathbf{a}_i\|} \geq \beta$ , where  $\|\mathbf{y}_i\| = \sqrt{\sum_i^k |\langle \mathbf{a}_i | \mathbf{v}_j \rangle|^2} \|\mathbf{a}_i\|$ .

Thanks to the this statement, it is possible to bound the run-time of Corollary 15 with a certain probability.

**Claim 19** (Quantum PCA on PCA-representable datasets). *Let  $\mathbf{a}_i$  be a row of  $\mathbf{A} \in \mathbb{R}^{n \times d}$ . Then, the runtime of Corollary 15 is  $\frac{\|\mathbf{a}_i\|}{\|\mathbf{y}_i\|} = \frac{1}{\beta} = O(1)$  with probability greater than  $\alpha$ .*

It is known that, in practical machine learning datasets,  $\alpha$  is a number fairly close to one. We have tested the value of  $\rho$  for the MNIST dataset, the interested reader can read more about it in the section about the experiments. Using the same framework and proof techniques, it is possible to produce similar results for the representations of CA and LSA.

*Remark:* Note that Yu et al. [62, Theorem 1] propose a lower bound for a quantity similar to  $\alpha$ . However, their result seems to be a loose bound: using their notation and setting  $\eta = 1, \theta = 1$  they bound this quantity with 0, while a tight bound should be 1.

## 4.2 Correspondence analysis

Correspondence analysis is a multivariate statistical tool, from the family of *factor analysis* methods, used to explore relationships among categorical variables. Consider two random variables  $X$  and  $Y$  with possible outcomes in  $\{x_1, \dots, x_n\}$  and  $\{y_1, \dots, y_m\}$  respectively, the model of Correspondence Analysis allows to represent the outcomes as vectors in two related Euclidean spaces. These spaces can be used for analysis purposes in data visualization, exploration and in other unsupervised machine learning tasks.

**Model** Given a contingency table for  $X$  and  $Y$ , it is possible to compute the matrix  $\mathbf{A} = \mathbf{D}_X^{-1/2} (\hat{\mathbf{P}}_{X,Y} - \hat{\mathbf{p}}_X \hat{\mathbf{p}}_Y^T) \mathbf{D}_Y^{-1/2} \in \mathbb{R}^{n \times m}$ , where  $\hat{\mathbf{P}}_{X,Y} \in \mathbb{R}^{n \times m}$  is the estimated matrix of joint probabilities,  $\hat{\mathbf{p}}_X \in \mathbb{R}^n$  and  $\hat{\mathbf{p}}_Y \in \mathbb{R}^m$  are the vectors of marginal probabilities, and  $\mathbf{D}_X^{-1/2} = \text{diag}(\hat{\mathbf{p}}_X)$ ,  $\mathbf{D}_Y^{-1/2} = \text{diag}(\hat{\mathbf{p}}_Y)$ . The computation of  $\mathbf{A}$  can be done in time proportional to the number of non zero entries of the contingency table. The singular value decomposition of  $\mathbf{A}$  is strictly related to the model of correspondence analysis [19, 26]. The vector space for  $X$  is  $\mathbf{D}_X^{-1/2} \mathbf{U} \in \mathbb{R}^{n \times k}$ , while the one for  $Y$  is  $\mathbf{D}_Y^{-1/2} \mathbf{V} \in \mathbb{R}^{m \times k}$ . Note that these spaces are not affected by the normalization of  $\mathbf{A}$ . Like in PCA, it is possible to choose only a subset of the orthogonal factors as coordinates for the representation. Factor scores and factor score ratios measure of how much “correspondence” is captured by the respective orthogonal factor, giving an estimate of the quality of the representation.

Similarly to what we have already discussed, it is possible to extract the model for CA by creating quantum access to the matrix  $\mathbf{A}$  and using Theorems 8, 9, and 11

to extract the orthogonal factors, the factor scores and the factor score ratios in time  $\tilde{O}\left(\left(\frac{1}{\gamma^2} + \frac{k(n+m)}{\theta\delta^2}\right)\frac{\mu(\mathbf{A})}{\epsilon}\right)$ . We provide a theoretical bound for the data representations in Lemma 20.

**Lemma 20** (Accuracy of  $\mathbf{D}_X^{-1/2}\mathbf{U}$  and  $\mathbf{D}_Y^{-1/2}\mathbf{V}$ ). *Let  $\mathbf{A} \in \mathbb{R}^{n \times m}$  be a matrix. Given some approximate procedures to retrieve unit estimates  $\bar{\mathbf{u}}_i$  of the left singular vectors  $\mathbf{u}_i$  such that  $\|\bar{\mathbf{u}}_i - \mathbf{u}_i\| \leq \delta$ , the error on  $\mathbf{D}_X^{-1/2}\mathbf{U}$  can be bounded as  $\|\mathbf{D}_X^{-1/2}\mathbf{U} - \mathbf{D}_X^{-1/2}\bar{\mathbf{U}}\|_F \leq \|\mathbf{D}_X^{-1/2}\|_F \sqrt{k}\delta$ . Similarly,  $\|\mathbf{D}_Y^{-1/2}\mathbf{V} - \mathbf{D}_Y^{-1/2}\bar{\mathbf{V}}\|_F \leq \|\mathbf{D}_Y^{-1/2}\|_F \sqrt{k}\delta$ .*

### 4.3 Latent semantic analysis

Latent semantic analysis is a data representation method to represent words and text documents as vectors in Euclidean spaces so that it is possible to make comparisons among terms, among documents and between terms and documents. The representation spaces of LSA automatically model synonymy and polysemy [12], and their applications in machine learning range from topic modeling to document clustering and retrieval.

**Model** The input of LSA is a contingency table of  $n$  words and  $m$  documents  $\mathbf{A} \in \mathbb{R}^{n \times m}$ . Inner products of rows  $\mathbf{A}\mathbf{A}^T = \mathbf{U}\Sigma^2\mathbf{U}^T$  express the distances between words. Inner products of columns  $\mathbf{A}^T\mathbf{A} = \mathbf{V}\Sigma^2\mathbf{V}^T$  express the distances between documents. The  $a_{ij}$  element of  $\mathbf{A} = \mathbf{U}\Sigma\mathbf{V}^T$  expresses the distance between word  $i$  and document  $j$ . With this definitions it is possible to compute: 1. a space for words comparisons  $\mathbf{U}\Sigma \in \mathbb{R}^{n \times k}$ ; 2. a space for documents comparisons  $\mathbf{V}\Sigma \in \mathbb{R}^{m \times k}$ ; 3. two spaces for words and documents comparisons  $\mathbf{U}\Sigma^{1/2} \in \mathbb{R}^{n \times k}$  and  $\mathbf{V}\Sigma^{1/2} \in \mathbb{R}^{m \times k}$ . When using LSA for latent semantic indexing, one wishes to represent the query as a vector in the document comparison space. The new vector is computed in the following way  $\mathbf{v}_q^T = \mathbf{x}_q^T \mathbf{U}\Sigma^{-1}$ , where  $\mathbf{x}_q \in \mathbb{R}^n$  is obtained using the same criteria used to store a document in  $\mathbf{A}$ . The orthogonal factors used to compare documents can be seen as latent topics whose importance is proportional to the corresponding factor score ratios.

As previously discussed, the cost of model extraction is  $\tilde{O}\left(\left(\frac{1}{\gamma^2} + \frac{k(n+m)}{\theta\delta^2}\right)\frac{\mu(\mathbf{A})}{\epsilon}\right)$ . In some applications, such as document retrieval, the data analyst maintains a fixed number of singular values and vectors, regardless of the factor score ratios. In Deerwester et al. [12],  $k = 100$  is found to be a good number for document indexing. Similarly, we believe that it is possible to empirically determine a threshold  $\theta$  to use in practice. Determining such threshold would reduce the complexity of model computation to the one of Theorem 11:  $\tilde{O}\left(\frac{k(n+m)}{\theta\delta^2}\frac{\mu(\mathbf{A})}{\epsilon}\right)$ .

For what concerns the error bounds on the retrieved data representation models, we already know from Lemma 13 that it is possible to retrieve an approximation  $\bar{\mathbf{U}}\Sigma$  and  $\bar{\mathbf{V}}\Sigma$  with precision  $\sqrt{k}(\delta + \epsilon)$ , where  $\delta$  is the precision on the singular vectors and  $\epsilon$  the precision on the singular values. To provide bounds on the estimations of  $\mathbf{U}\Sigma^{1/2}$ ,  $\mathbf{V}\Sigma^{1/2}$ , and  $\mathbf{U}\Sigma^{-1}$  we introduce Lemma 21 and Lemma 22.

**Lemma 21** (Accuracy of  $\bar{\mathbf{U}}\Sigma^{1/2}$  and  $\bar{\mathbf{V}}\Sigma^{1/2}$ ). *Let  $\mathbf{A} \in \mathbb{R}^{n \times m}$  be a matrix with  $\sigma_{\max} \leq 1$ . Given some approximate procedures to retrieve estimates  $\bar{\sigma}_i$  of the singular values  $\sigma_i$  such that  $\|\bar{\sigma}_i - \sigma_i\| \leq \epsilon$  and unitary estimates  $\bar{\mathbf{u}}_i$  of the left singular vectors  $\mathbf{u}_i$  such that  $\|\bar{\mathbf{u}}_i - \mathbf{u}_i\| \leq \delta$ , the error on  $\mathbf{U}\Sigma^{1/2}$  can be bounded as  $\|\mathbf{U}\Sigma^{1/2} - \bar{\mathbf{U}}\Sigma^{1/2}\|_F \leq \sqrt{k} \left(\delta + \frac{1}{2\sqrt{\theta}}\right)$ . Similarly,  $\|\mathbf{V}\Sigma^{1/2} - \bar{\mathbf{V}}\Sigma^{1/2}\|_F \leq \sqrt{k} \left(\delta + \frac{1}{2\sqrt{\theta}}\right)$ .*

**Lemma 22** (Accuracy of  $\overline{\mathbf{U}\Sigma}^{-1}$  and  $\overline{\mathbf{V}\Sigma}^{-1}$ ). *Let  $\mathbf{A} \in \mathbb{R}^{n \times m}$  be a matrix. Given some approximate procedures to retrieve estimates  $\bar{\sigma}_i$  of the singular values  $\sigma_i$  such that  $|\bar{\sigma}_i - \sigma_i| \leq \epsilon$  and unitary estimates  $\bar{\mathbf{u}}_i$  of the left singular vectors  $\mathbf{u}_i$  such that  $\|\bar{\mathbf{u}}_i - \mathbf{u}_i\| \leq \delta$ , the error on  $\mathbf{U}\Sigma^{-1}$  can be bounded as  $\|\mathbf{U}\Sigma^{-1} - \overline{\mathbf{U}\Sigma}^{-1}\|_F \leq \sqrt{k} \left( \frac{\delta}{\theta} + \frac{\epsilon}{\theta^2 - \theta\epsilon} \right)$ . Similarly,  $\|\mathbf{V}\Sigma^{-1} - \overline{\mathbf{V}\Sigma}^{-1}\|_F \leq \sqrt{k} \left( \frac{\delta}{\theta} + \frac{\epsilon}{\theta^2 - \theta\epsilon} \right)$ .*

The interested reader can find the formal statements and proofs for the bounds of the non-normalized representations in the appendix.

## 5 Experiments

We have analysed the distribution of the factor score ratios in the MNIST, Fashion MNIST, CIFAR-10 and Research Papers datasets. They decrease fast (figures are included in the appendix), confirming the low rank nature of the data. Focusing on MNIST, Fashion-MNIST, and CIFAR-10 we have simulated PCA’s dimensionality reduction for image classification. The datasets have been shifted to row mean 0 and normalized them so that  $\sigma_{\max} = 1$ . We have simulated Algorithm 1 by sampling  $1/\gamma^2 = 1000$  times from the state  $\sum_i^r \lambda_i |\mathbf{u}_i\rangle |\mathbf{v}_i\rangle |\bar{\sigma}_i\rangle$  to search the first  $k$  principal components that account for a factor score ratios sum  $p = 0.85$ . In all cases, sampling the singular values has been enough to decide how many to keep. However, as  $p$  increases, the gap between the factor score ratios decreases and the quality of the estimation of  $k$  or  $\theta$  decreases. As discussed in Section 3.1, it is possible to detect this problem using Theorem 9, and solve it with a binary search for  $\theta$ . We have tested the quality of the representation by observing the accuracy of 10-fold cross-validation k-nearest neighbors with  $k = 7$  as we introduce error in the representation’s Frobenius norm (see Figure 1). To introduce the error we have added truncated Gaussian noise to each element of  $\mathbf{U}\Sigma$  to have  $\|\mathbf{U}\Sigma - \overline{\mathbf{U}\Sigma}\| \leq \xi = \sqrt{k}(\epsilon + \delta)$  (Lemma 13). The parameter  $\delta$  has been estimated using the bound above, choosing the error so that the accuracy drops no more than 0.01, and fixing  $\epsilon$  to the greatest between the one that preserves the ordering of the singular values and the one that allows for correct thresholding. The run-time parameters are summarized in Table 1. The results show that Theorems 8, 9, 10 are already advantageous on a small datasets, while Theorem 11 requires bigger datasets to express its speed-up. We have also simulated the creation of the state at step 6 of Algorithm 2 to test the average number of measurements needed to collect all the singular values as  $\epsilon$  increases. The analysis has confirmed the run-time’s expectations. To end with, we have tested the value of  $\alpha$  (Definition 18, Claim 19) for the MNIST dataset, fixing  $\epsilon = 0$  and trying  $p \in \{0.1, 0.2, 0.3, 0.4, 0.5, 0.6, 0.7, 0.8, 0.9\}$ . We have observed that  $\alpha = 0.96 \pm 0.02$ , confirming that the run-time of Corollary 15 can be assumed constant for the majority of the data points of a PCA-representable dataset. We also point out that more experiments on the run-time parameters have been extensively discussed in many other works that rely on the same techniques [28, 35]. These works study the scaling of the parameters dataset’s size increases, both in features and samples, and conclude that the parameters of interest are almost constant.

## 6 Conclusions

We formulate many eigenvalue problems in machine learning within a useful framework, bridging the gap left open by previous literature. Our new procedures fill the gap by estimating the quality of a representation and extracting a classical description of the top-k

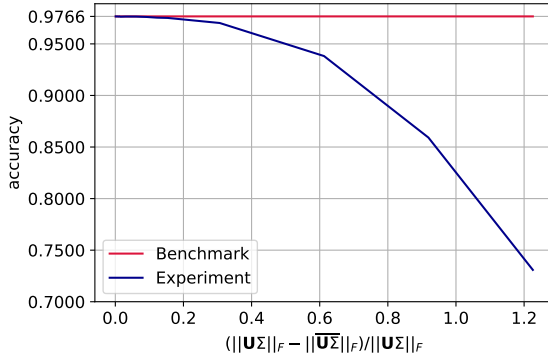


Figure 1: Accuracy of 10-fold cross-validation using K-Nearest-Neighbors, with 7 neighbors, on the MNIST dataset after PCA’s dimensionality reduction (0.8580% of variance retained). The *benchmark* accuracy was computed with an exact PCA. The *experiment* line shows how the classification accuracy decreases as error is introduced in the Frobenius norm of the representation.

Table 1: Summary of the run-time parameters. The parameters that depend on  $k$  have been computed using the estimated  $k$ .

PARAMETER	MNIST	F-MNIST	CIFAR-10
$\ \mathbf{A}\ _F$	3.2032	1.8551	1.8540
$\mu(\mathbf{A}) = \ \mathbf{A}\ _\infty$	0.3730	0.3207	0.8710
ESTIMATED $k$	62	45	55
EXACT $k$	59	43	55
ESTIMATED $p$	0.8510	0.8510	0.8510
EXACT $p$	0.8580	0.8543	0.8514
ORDR. $\epsilon$	0.0003	0.0003	0.0002
THRS. $\epsilon$	0.0030	0.0009	0.0006
$\theta$	0.1564	0.0776	0.0746
$\delta$	0.1124	0.0106	0.0340

singular values and vectors. We have shown how to use the new tools to extract the information needed by SDV-based data representation algorithms, computing theoretical error bounds for three machine learning applications. The new algorithms to extract the models for PCA, CA, and LSA are beneficial in scenarios where a central server computes the model and distributes it to various endpoints. By creating quantum states of the representation, we allow deeper machine learning pipelines in the quantum feature space. We provide experiments for PCA’s dimensionality reduction to better show how the procedures can be used. Besides identifying the proper quantum tools and formalizing the novel quantum algorithms, the main technical difficulty was analyzing how the error propagates to the bounds and run-times. We do not provide circuit implementations of our procedures as they can be easily designed using circuits that have been widely discussed in quantum computing literature.

We do not expect further run-time improvements that exceed poly-logarithmic factors or constant factors given by circuital implementations. For non-zero singular values and dense singular vectors, the run-time of the extraction can not be smaller than  $kz$ , as one needs to read vectors of size  $kz$ . The  $\delta^2$  parameter is a tight bound for the  $\ell_2$  norm of the

vectors, as it is a result of Chernoff’s bound. The parameter  $\epsilon$  is a tight error bound from phase estimation, which is necessary to separate the singular vectors.  $\theta$  is the condition number of the low-rank approximation of the matrix, and it is necessary to amplify the amplitudes of the smallest singular values.

**Future works** We deem interesting to explore quantum algorithms for incremental SVD, for dataset’s whose points are available as a streaming of data. Finally, for algorithms whose aim is to obtain a representation, with little interest on the classical description of the model, it would be interesting to investigate how the block-encoding and singular value transformation frameworks [8, 15] can speed-up the creation of quantum states proportional to the dataset representation. However, this approach would have the drawback of introducing a multiplicative term in the run-times of subsequent quantum machine learning algorithms.

## 7 Acknowledgements

A.L. is supported by QuantERA ERA-NET Cofund in Quantum Technologies implemented within the European Union’s Horizon 2020 Programme (QuantAlgo project), the ANRT, and Singapore’s National Research Foundation, the Prime Minister’s Office, Singapore, the Ministry of Education, Singapore under the Research Centres of Excellence program under research grant R 710-000-012-135.

## References

- [1] Jonathan Alcock, Chang-Yu Hsieh, Iordanis Kerenidis, and Shengyu Zhang. Quantum algorithms for feedforward neural networks. *ACM Transactions on Quantum Computing*, 1(1):1–24, 2020.
- [2] Juan Miguel Arrazola, Alain Delgado, Bhaskar Roy Bardhan, and Seth Lloyd. Quantum-inspired algorithms in practice. *Quantum*, 4:307, 2020. DOI: [10.22331/q-2020-08-13-307](https://doi.org/10.22331/q-2020-08-13-307).
- [3] Jacob Biamonte, Peter Wittek, Nicola Pancotti, Patrick Rebentrost, Nathan Wiebe, and Seth Lloyd. Quantum machine learning. *Nature*, 549(7671):195–202, 2017. DOI: [10.1038/nature23474](https://doi.org/10.1038/nature23474).
- [4] Gilles Brassard, Peter Hoyer, Michele Mosca, and Alain Tapp. Quantum amplitude amplification and estimation. *Contemporary Mathematics*, 305:53–74, 2002. DOI: [10.1090/conm/305/052152](https://doi.org/10.1090/conm/305/052152).
- [5] Carlos Bravo-Prieto, Diego García-Martín, and José I Latorre. Quantum singular value decomposer. *Physical Review A*, 101(6):062310, 2020. DOI: [10.1103/PhysRevA.101.062310](https://doi.org/10.1103/PhysRevA.101.062310).
- [6] Chris Cade and Ashley Montanaro. The quantum complexity of computing schatten  $p$ -norms. *arXiv preprint arXiv:1706.09279*, 2017.
- [7] Joseph M Cavanagh, Thomas E Potok, and Xiaohui Cui. Parallel latent semantic analysis using a graphics processing unit. In *Proceedings of the 11th Annual Conference Companion on Genetic and Evolutionary Computation Conference: Late Breaking Papers*, pages 2505–2510, 2009. DOI: [10.1145/1570256.1570352](https://doi.org/10.1145/1570256.1570352).
- [8] Shantanav Chakraborty, András Gilyén, and Stacey Jeffery. The Power of Block-Encoded Matrix Powers: Improved Regression Techniques via Faster Hamiltonian Simulation. In *46th International Colloquium on Automata, Languages, and Programming (ICALP 2019)*, volume 132 of *Leibniz International Proceedings in Informatics*

(LIPICs), pages 33:1–33:14. Schloss Dagstuhl–Leibniz-Zentrum fuer Informatik, 2019. ISBN 978-3-95977-109-2. DOI: [10.4230/LIPIcs.ICALP.2019.33](https://doi.org/10.4230/LIPIcs.ICALP.2019.33).

[9] Nadiia Chepurko, Kenneth L Clarkson, Lior Horesh, and David P Woodruff. Quantum-inspired algorithms from randomized numerical linear algebra. 2020.

[10] Nai-Hui Chia, András Gilyén, Tongyang Li, Han-Hsuan Lin, Ewin Tang, and Chunhao Wang. Sampling-based sublinear low-rank matrix arithmetic framework for dequantizing quantum machine learning. In *Proceedings of the 52nd Annual ACM SIGACT Symposium on Theory of Computing*, pages 387–400, 2020. DOI: [10.1145/3357713.3384314](https://doi.org/10.1145/3357713.3384314).

[11] Sten Erik Clausen. *Applied correspondence analysis: An introduction*, volume 121. Sage, 1998. DOI: [10.4135/9781412983426](https://doi.org/10.4135/9781412983426).

[12] Scott Deerwester, Susan T Dumais, George W Furnas, Thomas K Landauer, and Richard Harshman. Indexing by latent semantic analysis. *Journal of the American society for information science*, 41(6):391–407, 1990. DOI: [10.1002/\(SICI\)1097-4571\(199009\)41:6<391::AID-ASI1>3.0.CO;2-9](https://doi.org/10.1002/(SICI)1097-4571(199009)41:6<391::AID-ASI1>3.0.CO;2-9).

[13] Paul Erdős. On a classical problem of probability theory. 1961.

[14] Alan Frieze, Ravi Kannan, and Santosh Vempala. Fast monte-carlo algorithms for finding low-rank approximations. *Journal of the ACM (JACM)*, 51(6):1025–1041, 2004. DOI: [10.1145/1039488.1039494](https://doi.org/10.1145/1039488.1039494).

[15] András Gilyén, Yuan Su, Guang Hao Low, and Nathan Wiebe. Quantum singular value transformation and beyond: exponential improvements for quantum matrix arithmetics. In *Proceedings of the 51st Annual ACM SIGACT Symposium on Theory of Computing*, pages 193–204, 2019. DOI: [10.1145/3313276.3316366](https://doi.org/10.1145/3313276.3316366).

[16] András Gilyén, Zhao Song, and Ewin Tang. An improved quantum-inspired algorithm for linear regression. *arXiv preprint arXiv:2009.07268*, 2020.

[17] Fabio A. González and Juan C. Caicedo. Quantum latent semantic analysis. In Giambattista Amati and Fabio Crestani, editors, *Advances in Information Retrieval Theory*, pages 52–63, Berlin, Heidelberg, 2011. Springer Berlin Heidelberg. ISBN 978-3-642-23318-0. DOI: [10.1007/978-3-642-23318-0\\_7](https://doi.org/10.1007/978-3-642-23318-0_7).

[18] Michael Greenacre. *Correspondence analysis in practice*. CRC press, 2017. DOI: [10.1201/9781315369983](https://doi.org/10.1201/9781315369983).

[19] Michael J Greenacre. Theory and applications of correspondence analysis. 1984.

[20] Lejia Gu, Xiaoqiang Wang, and Guofeng Zhang. Quantum higher order singular value decomposition. In *2019 IEEE International Conference on Systems, Man and Cybernetics (SMC)*, pages 1166–1171. IEEE, 2019. DOI: [10.1109/SMC.2019.8914525](https://doi.org/10.1109/SMC.2019.8914525).

[21] Casper Gyurik, Chris Cade, and Vedran Dunjko. Towards quantum advantage for topological data analysis. *arXiv preprint arXiv:2005.02607*, 2020.

[22] Nathan Halko, Per-Gunnar Martinsson, Yoel Shkolnisky, and Mark Tygert. An algorithm for the principal component analysis of large data sets. *SIAM Journal on Scientific computing*, 33(5):2580–2594, 2011. DOI: [10.1016/S0169-7439\(01\)00130-7](https://doi.org/10.1016/S0169-7439(01)00130-7).

[23] Aram W Harrow, Avinatan Hassidim, and Seth Lloyd. Quantum algorithm for linear systems of equations. *Physical review letters*, 103(15):150502, 2009. DOI: [10.1103/PhysRevLett.103.150502](https://doi.org/10.1103/PhysRevLett.103.150502).

[24] Harun-Ur-Rashid. Research paper dataset, 2018. URL <https://www.kaggle.com/harunshimanto/research-paper>.

[25] Chen He, Jiazen Li, and Weiqi Liu. An exact quantum principal component analysis algorithm based on quantum singular value threshold. *arXiv preprint arXiv:2010.00831*, 2020.

[26] Hsiang Hsu, Salman Salamatian, and Flavio P Calmon. Correspondence analysis using neural networks. In *The 22nd International Conference on Artificial Intelligence and Statistics*, pages 2671–2680, 2019.

[27] Ian T Jolliffe and Jorge Cadima. Principal component analysis: a review and recent developments. *Philosophical Transactions of the Royal Society A: Mathematical, Physical and Engineering Sciences*, 374(2065):20150202, 2016. DOI: [10.1098/rsta.2015.0202](https://doi.org/10.1098/rsta.2015.0202).

[28] Iordanis Kerenidis and Alessandro Luongo. Classification of the mnist data set with quantum slow feature analysis. *Physical Review A*, 101(6):062327, 2020. DOI: [10.1103/PhysRevA.101.062327](https://doi.org/10.1103/PhysRevA.101.062327).

[29] Iordanis Kerenidis and Anupam Prakash. Quantum recommendation systems. In *8th Innovations in Theoretical Computer Science Conference (ITCS 2017)*. Schloss Dagstuhl-Leibniz-Zentrum fuer Informatik, 2017. DOI: [10.4230/LIPIcs.ITCS.2017.49](https://doi.org/10.4230/LIPIcs.ITCS.2017.49).

[30] Iordanis Kerenidis and Anupam Prakash. A quantum interior point method for lps and sdps. *ACM Transactions on Quantum Computing*, 1(1):1–32, 2020. DOI: [10.1145/3406306](https://doi.org/10.1145/3406306).

[31] Iordanis Kerenidis and Anupam Prakash. Quantum gradient descent for linear systems and least squares. *Physical Review A*, 101(2):022316, 2020. DOI: [10.1103/PhysRevA.101.022316](https://doi.org/10.1103/PhysRevA.101.022316).

[32] Iordanis Kerenidis, Jonas Landman, Alessandro Luongo, and Anupam Prakash. q-means: A quantum algorithm for unsupervised machine learning. In *Advances in Neural Information Processing Systems*, pages 4134–4144, 2019.

[33] Iordanis Kerenidis, Jonas Landman, and Anupam Prakash. Quantum algorithms for deep convolutional neural networks. In *International Conference on Learning Representations*, 2019.

[34] Iordanis Kerenidis, Anupam Prakash, and Dániel Szilágyi. Quantum algorithms for portfolio optimization. In *Proceedings of the 1st ACM Conference on Advances in Financial Technologies*, pages 147–155, 2019. DOI: [10.1145/3318041.3355465](https://doi.org/10.1145/3318041.3355465).

[35] Iordanis Kerenidis, Alessandro Luongo, and Anupam Prakash. Quantum expectation-maximization for gaussian mixture models. In *International Conference on Machine Learning*, pages 5187–5197. PMLR, 2020.

[36] Iordanis Kerenidis, Alessandro Luongo, and Anupam Prakash. Quantum expectation-maximization for gaussian mixture models. In *International Conference on Machine Learning*, pages 5187–5197. PMLR, 2020.

[37] Naoko Koide-Majima and Kei Majima. Quantum-inspired canonical correlation analysis for exponentially large dimensional data. *Neural Networks*, 135:55–67, 2021. ISSN 0893-6080. DOI: [10.1016/j.neunet.2020.11.019](https://doi.org/10.1016/j.neunet.2020.11.019).

[38] Alex Krizhevsky et al. Learning multiple layers of features from tiny images. 2009.

[39] Thomas K Landauer, Danielle S McNamara, Simon Dennis, and Walter Kintsch. *Handbook of latent semantic analysis*. Psychology Press, 2013. DOI: [10.4324/9780203936399](https://doi.org/10.4324/9780203936399).

[40] Yann LeCun, Léon Bottou, Yoshua Bengio, and Patrick Haffner. Gradient-based learning applied to document recognition. *Proceedings of the IEEE*, 86(11):2278–2324, 1998. DOI: [10.1109/5.726791](https://doi.org/10.1109/5.726791).

[41] Richard B Lehoucq, Danny C Sorensen, and Chao Yang. *ARPACK users' guide: solution of large-scale eigenvalue problems with implicitly restarted Arnoldi methods*. SIAM, 1998. DOI: [10.1137/1.9780898719628](https://doi.org/10.1137/1.9780898719628).

[42] Jie Lin, Wan-Su Bao, Shuo Zhang, Tan Li, and Xiang Wang. An improved quantum principal component analysis algorithm based on the quantum sin-

gular threshold method. *Physics Letters A*, 383(24):2862–2868, 2019. DOI: [10.1016/j.physleta.2019.06.026](https://doi.org/10.1016/j.physleta.2019.06.026).

[43] Seth Lloyd, Masoud Mohseni, and Patrick Rebentrost. Quantum principal component analysis. *Nature Physics*, 10(9):631–633, 2014. DOI: [10.1038/nphys3029](https://doi.org/10.1038/nphys3029).

[44] Guang Hao Low and Isaac L Chuang. Hamiltonian simulation by qubitization. *Quantum*, 3:163, 2019. DOI: [10.22331/q-2019-07-12-163](https://doi.org/10.22331/q-2019-07-12-163).

[45] Carlos Ortiz Marrero, Mária Kieferová, and Nathan Wiebe. Entanglement induced barren plateaus. *arXiv preprint arXiv:2010.15968*, 2020.

[46] Matthew Partridge and Rafael Calvo. Fast dimensionality reduction and simple pca. *Intelligent data analysis*, 2(3):292–298, 1997. DOI: [10.3233/IDA-1998-2304](https://doi.org/10.3233/IDA-1998-2304).

[47] F. Pedregosa, G. Varoquaux, A. Gramfort, V. Michel, B. Thirion, O. Grisel, M. Blondel, P. Prettenhofer, R. Weiss, V. Dubourg, J. Vanderplas, A. Passos, D. Cournapeau, M. Brucher, M. Perrot, and E. Duchesnay. Scikit-learn: Machine learning in Python. *Journal of Machine Learning Research*, 12:2825–2830, 2011.

[48] Patrick Rebentrost, Masoud Mohseni, and Seth Lloyd. Quantum support vector machine for big data classification. *Physical review letters*, 113(13):130503, 2014.

[49] Patrick Rebentrost, Masoud Mohseni, and Seth Lloyd. Quantum support vector machine for big data classification. *Physical review letters*, 113(13):130503, 2014. DOI: [10.1103/PhysRevLett.113.130503](https://doi.org/10.1103/PhysRevLett.113.130503).

[50] Patrick Rebentrost, Adrian Steffens, Iman Marvian, and Seth Lloyd. Quantum singular-value decomposition of nonsparse low-rank matrices. *Physical review A*, 97(1):012327, 2018. DOI: [10.1103/PhysRevA.97.012327](https://doi.org/10.1103/PhysRevA.97.012327).

[51] Youcef Saad. *Numerical methods for large eigenvalue problems*. Manchester University Press, 1992. DOI: [10.1137/1.9781611970739](https://doi.org/10.1137/1.9781611970739).

[52] Maria Schuld and Francesco Petruccione. *Supervised Learning with Quantum Computers*. Springer, 2018. ISBN ISBN 978-3-319-96423-2. DOI: [10.1007/978-3-319-96424-9](https://doi.org/10.1007/978-3-319-96424-9).

[53] Danny C Sorensen. Implicitly restarted arnoldi/lanczos methods for large scale eigenvalue calculations. In *Parallel Numerical Algorithms*, pages 119–165. Springer, 1997. DOI: [10.1007/978-94-011-5412-3\\_5](https://doi.org/10.1007/978-94-011-5412-3_5).

[54] Ewin Tang. A quantum-inspired classical algorithm for recommendation systems. In *Proceedings of the 51st Annual ACM SIGACT Symposium on Theory of Computing*, pages 217–228, 2019. DOI: [10.1145/3313276.3316310](https://doi.org/10.1145/3313276.3316310).

[55] Guoming Wang. Quantum algorithm for linear regression. *Physical review A*, 96(1):012335, 2017.

[56] Hao Wang, Lisa Vo, Flavio P Calmon, Muriel Médard, Ken R Duffy, and Mayank Varia. Privacy with estimation guarantees. *IEEE Transactions on Information Theory*, 65(12):8025–8042, 2019. DOI: [10.1109/TIT.2019.2934414](https://doi.org/10.1109/TIT.2019.2934414).

[57] Samson Wang, Enrico Fontana, Marco Cerezo, Kunal Sharma, Akira Sone, Lukasz Cincio, and Patrick Coles. Noise-induced barren plateaus in variational quantum algorithms. *Bulletin of the American Physical Society*, 2020.

[58] Xin Wang, Zhixin Song, and Youle Wang. Variational quantum singular value decomposition. *arXiv*, pages arXiv–2006, 2020.

[59] Xuansheng Wang, Beidun Chen, Jianqiang Sheng, Hongying Zheng, Tangren Dan, and Xianfeng Wu. An improved lanczos algorithm for principal component analysis. In *Proceedings of 2020 the 6th International Conference on Computing and Data Engineering*, pages 70–74, 2020. DOI: [10.1145/3379247.3379250](https://doi.org/10.1145/3379247.3379250).

[60] Han Xiao, Kashif Rasul, and Roland Vollgraf. Fashion-mnist: a novel image dataset for benchmarking machine learning algorithms. *arXiv preprint cs.LG/1708.07747*, 2017.

- [61] Bo Yu, Zong-ben Xu, and Cheng-hua Li. Latent semantic analysis for text categorization using neural network. *Knowledge-Based Systems*, 21(8):900–904, 2008. DOI: [10.1016/j.knosys.2008.03.045](https://doi.org/10.1016/j.knosys.2008.03.045).
- [62] Chao-Hua Yu, Fei Gao, Song Lin, and Jingbo Wang. Quantum data compression by principal component analysis. *Quantum Information Processing*, 18(8):249, 2019. DOI: [10.1007/s11128-019-2364-9](https://doi.org/10.1007/s11128-019-2364-9).
- [63] Mingxi Zhang, Pohan Li, and Wei Wang. An index-based algorithm for fast on-line query processing of latent semantic analysis. *PLoS One*, 12(5):e0177523, 2017. DOI: [10.1371/journal.pone.0177523](https://doi.org/10.1371/journal.pone.0177523).
- [64] Radim Řehůřek. Subspace tracking for latent semantic analysis. In *European Conference on Information Retrieval*, pages 289–300. Springer, 2011. DOI: [10.1007/978-3-642-20161-5\\_29](https://doi.org/10.1007/978-3-642-20161-5_29).

## A Extended related works

One of the first papers that faced the problem of performing the eigendecomposition of a matrix with a quantum computer is the well-known Lloyd et al. [43], which leveraged the intuition that density matrices are covariance matrix whose trace has been normalized. In this work, the authors assume to have quantum access to a matrix in the form of a density matrix and develop a method for fast density matrix exponentiation that allows preparing the eigendecomposition of the full input matrix in time logarithmic on its dimensions. However, this algorithm requires the input matrix to be square, symmetric, and sparse or low-rank. More recently, the works of Kerenidis et al. on recommendation systems [29] and least-squares [31] have used a different definition of quantum access to a matrix (the one used throughout this work) and defined the task of singular value estimation. Their singular value decomposition scales better with respect to the error parameters, eliminates the dependency on the condition number and does not require the input matrix to be square, symmetric and sparse or low-rank. Several recent works, such as Gu et al. [20], Lin et al. [42], Rebentrost et al. [50], have tried to improve or to extend the quantum singular value decomposition techniques, almost none of them have provided a formal analysis of an algorithm that allows classical access to singular values, singular vectors and amount of variance explained by each. In the last few months, there have been attempts at creating near-term quantum algorithms for singular value decomposition. The authors of these works propose quantum circuits for singular value decomposition of quantum states on noisy intermediate-scale quantum (NISQ) devices using variational circuits [5, 58]. However, the complexity of such methods is still not clear and recent works have questioned the efficacy of the speed-ups of variational quantum algorithms due to (entanglement and noise-induced) barren plateaus in the optimization landscape that often nullify the speed-ups [45, 57].

The realization of quantum procedures that provide exponential speed-ups in linear algebra tasks has given inspiration for the realization of classical quantum-inspired algorithms that try to achieve the same run-time as their quantum counterparts. The process of transforming a quantum algorithm in a classical algorithm with a similar speed-up is usually referred to as “de-quantization”. Often, the comparison with dequantized algorithms is not easy, as they solve problems that are different from ours. Most of these works are based on a famous algorithm by Frieze, Kannan, and Vempala which computes a low-rank approximation of a matrix in time which is sub-linear in the number of its elements [2, 10, 14]. Such algorithms promise exponential speed-ups over the traditional SVD algorithm for low-rank matrices. However, the high polynomial dependency of the run-times on the condition number, the rank, and the estimation error makes them advantageous only for matrices of extremely large dimensions, with low ranks and small condition numbers. The research described in Arrazola et al. [2] observed that the dependencies like  $O\left(\frac{\|A\|_F^6}{\epsilon^6}\right)$  are far from being tight in real implementations, but still order of magnitudes slower than the best classical algorithms.

Concomitantly to our work, a new important result [9] was able to lower the complexity of these dequantization by better leveraging all the previous literature of classical algorithms in randomized linear algebra, and re-framing them into a more complete mathematical framework. In fact, as noted previous sample-based dequantizations were just doing a form of leverage score sampling. These new algorithms seem to be tighter than previous results, and offer better comparison with quantum algorithms, solving problems that are related to ours. While we believe that it is not possible have classical algorithms with run-times comparable to the ones of Theorems 8, 9, 10 (see the relationships between

LLSD, SUES and DQC1 in Cade and Montanaro [6]) and Corollaries 15 and 16, we have found that the work of Chepurko et al. [9] may question the practical advantage of our Theorem 11 over a classical counterpart. At a first sight their Theorem 33 might seem relevant for this work, as it provides a set of linear independent rows of the input matrix. We stress that this problem is not related to finding the singular vectors provided by SVD, which are not only linearly independent but also orthonormal. Moreover, even after further orthonormalization processing (e.g. Gram–Schmidt), the computed row basis wouldn't necessarily be the one provided by SVD. This is why the run-time of this procedure cannot be compared to our Theorem 11. On the other hand, Theorem 37 is more similar to our Theorem 11, but still aims to solve a different problem. While ours provides estimates  $\|v_i - \bar{v}_i\| \leq \epsilon, \forall i \in [k]$  (which we recall are also relative-error estimates, as  $\|v_i\| = 1$ ), their Theorem 37 provides a rank- $k$  projector matrix  $Q^{(k)}$ , with orthonormal columns, such that  $\|A - AQ^{(k)}Q^{(k)T}\|_F^2 \leq (1 + \epsilon')\|A - A_k\|_F^2$  in time  $\tilde{O}(nnz(\mathbf{A}) + \frac{k^{w-1}m}{\epsilon'} + \frac{k^{1.01}m}{\epsilon'^2})$ . While it is easy to see that  $Q \rightarrow V$  as  $\epsilon \rightarrow 0$ , it is not easy to see how  $\|\mathbf{Q} - \mathbf{V}\|_F$  varies as  $\epsilon$  varies and that becomes even less clear if we are interested in the error on a specific singular vector. If the run-time of this algorithm is shown to be better than its quantum equivalent, it would still be great to include it in our framework instead of Theorem 11 and continue to take advantage of the speed-ups of the other quantum procedures. One downside of using the de-quantized subroutines would be that, in general, the  $\tilde{O}(nnz(\mathbf{A}))$  data pre-processing step is different from the one required to provide efficient quantum access. Even though it can be possible that a classical algorithm could extract the singular vectors with a run-time comparable to the quantum one, using it would require paying additional costs both in time and space. Those costs arise from the need for an ad hoc data structure that would not be adequate to provide competitive speed-ups with respect to the other available quantum machine learning and data analysis algorithms. We believe that it is possible that both the classical and quantum versions of singular vectors extraction will be used in the future, depending on the computational capabilities available to the interested data analysts.

Computationally, most diffused implementations of PCA, CA, and LSA available [47] relays on ARPACK [41] or similar packages, which implement improvements of the Lanczos method, like the Implicitly restarted Arnoldi method (IRAM) [53], an improvement upon the simple Arnoldi iteration, which dates back to 1951 (a more general case of Lanczos algorithm, which works only for Hermitian matrices). The runtime of these algorithm is bounded by  $O(nmk \frac{\ln(m/\epsilon)}{\sqrt{\epsilon}})$ , where  $\epsilon$  is an approximation error related to the relative spectral gap between eigenvalues [51].

**PCA.** Probably no other algorithm in ML has been studied as much as PCA, so the literature around this algorithm is vast [22, 27]. To mention an improvement upon the standard Lanczos method for PCA [59], the authors basically used more Lanczos iterations to improve the numerical stability of PCA, by obtaining a better description of the Krylov subspace (i.e. more iterations help obtaining a more orthonormal base). As mentioned, the problem of PCA has been studied previously within the model of quantum computation. He et al. [25], Lin et al. [42] focus on a circuit implementation of qPCA, whose run-time is over-seeded by more recent techniques used in this paper. The work of Yu et al. [62] face the problem of performing PCA for dimensionality reduction on quantum states achieving an exponential advantage over the best known classical algorithms. However, their algorithm is somewhat impractical, due to the overall error dependence, which can be of  $\tilde{O}(\epsilon^{-5})$ . Furthermore they use old Hamiltonian simulation techniques, which are super-seeded by the techniques that we use in our paper. To our knowledge, there are

no works that provide a theoretical analysis of the run-time for the procedure needed to *select* the number of singular vectors needed to retain enough variance, obtain a classical description of the model, and map new data points in the new feature space with theoretical guarantees on the runtime (which we believe cannot be improved, as in this work we show that the run-time for this mapping is almost constant).

**CA.** While correspondence analysis has been really popular in the past, so much that entire books have been written about it [11, 18], it seems to be went out of fashion the last decades, probably overshadowed by the wave of results in deep-learning. A new perspective of CA is given by the novel formulation of Hsu et al. [26], where the authors connects correspondence analysis to the principal inertia components theory, making it relevant also in tasks that concern privacy in machine learning [56]. As said before, similarly and independently from us, Koide-Majima and Majima [37] have extended the de-quantized subroutines to perform canonical correspondence analysis. This algorithms is not expected to beat the performance of our quantum algorithm, let alone the performance of the best classical algorithm for CA.

**LSA.** LSA was first introduced in Deerwester et al. [12], which spurred a flurry of applications [39]. Some notable works are a streaming and/or distributed algorithm for incremental LSA [7, 63, 64]. While this work might offer inspiration for new quantum algorithms, the distributed nature of this work make it an unfair comparison with a single-QPU quantum algorithm. LSA with neural networks has also been explored in the past years [61], albeit without guarantees on the run-time or the approximation error. During the preparation of this manuscript we discovered the existence of a previous work on quantum LSA, which pointed at the similarities between quantum states and LSA, albeit without offering any algorithm for doing it [17].

## B Algorithms and proofs

Before reporting the proofs, we state the two Claims for the non-normalized LSA representations.

**Claim 23** (Non-normalized  $\bar{\mathbf{U}}\Sigma^{1/2}$  and  $\bar{\mathbf{V}}\Sigma^{1/2}$ ). *The estimated representations of Lemma 21, for the not-normalized matrix  $\mathbf{A}$ , are  $\sqrt{\|\mathbf{A}\|} \bar{\mathbf{U}}\Sigma^{1/2}$  and  $\sqrt{\|\mathbf{A}\|} \bar{\mathbf{V}}\Sigma^{1/2}$ . The error bounds become  $\left\| \sqrt{\|\mathbf{A}\|} \bar{\mathbf{U}}\Sigma^{1/2} - \sqrt{\|\mathbf{A}\|} \mathbf{U}\Sigma^{1/2} \right\|_F \leq \sqrt{k\|\mathbf{A}\|}(\epsilon + \delta)$  and  $\left\| \sqrt{\|\mathbf{A}\|} \bar{\mathbf{V}}\Sigma^{1/2} - \sqrt{\|\mathbf{A}\|} \mathbf{V}\Sigma^{1/2} \right\|_F \leq \sqrt{k\|\mathbf{A}\|}(\epsilon + \delta)$ .*

**Claim 24** (Non-normalized  $\bar{\mathbf{U}}\Sigma^{-1}$  and  $\bar{\mathbf{V}}\Sigma^{-1}$ ). *The estimated representations of Lemma 22, for the not-normalized matrix  $\mathbf{A}$ , are  $\frac{1}{\|\mathbf{A}\|} \bar{\mathbf{U}}\Sigma^{-1}$  and  $\frac{1}{\|\mathbf{A}\|} \bar{\mathbf{V}}\Sigma^{-1}$ . The error bounds become  $\left\| \frac{1}{\|\mathbf{A}\|} \bar{\mathbf{U}}\Sigma^{-1} - \frac{1}{\|\mathbf{A}\|} \mathbf{U}\Sigma^{1/2} \right\| \leq \frac{\sqrt{k}}{\|\mathbf{A}\|} \left( \frac{\delta}{\theta} + \frac{\epsilon}{\theta^2 - \theta\epsilon} \right)$  and  $\left\| \frac{1}{\|\mathbf{A}\|} \bar{\mathbf{V}}\Sigma^{-1} - \frac{1}{\|\mathbf{A}\|} \mathbf{V}\Sigma^{1/2} \right\| \leq \frac{\sqrt{k}}{\|\mathbf{A}\|} \left( \frac{\delta}{\theta} + \frac{\epsilon}{\theta^2 - \theta\epsilon} \right)$ .*

We also provide a useful claim that will be used to bound errors on quantum states.

**Claim 25** (Closeness of state-vectors [31]). *Let  $\theta$  be the angle between vectors  $\mathbf{x}, \bar{\mathbf{x}}$  and assume that  $\theta < \pi/2$ . Then,  $\|\mathbf{x} - \bar{\mathbf{x}}\| \leq \epsilon$  implies  $\|\lvert \mathbf{x} \rangle - \lvert \bar{\mathbf{x}} \rangle\| \leq \sqrt{2} \frac{\epsilon}{\|\mathbf{x}\|}$ .*

---

**Algorithm 1** Quantum factor score ratio estimation.

---

- 1:  $S = 0$
- 2: **while**  $S < \tilde{O}\left(\frac{1}{\gamma^2}\right)$  **do**
- 3:     Prepare the state  $\frac{1}{\|\mathbf{A}\|_F} \sum_i^n \sum_j^m a_{ij} |i\rangle |j\rangle$ .
- 4:     Apply SVE to get  $\frac{1}{\sqrt{\sum_j^r \sigma_j^2}} \sum_i^r \sigma_i |\mathbf{u}_i\rangle |\mathbf{v}_i\rangle |\bar{\sigma}_i\rangle$ .
- 5:     Measure the last register and store a counter of how many times each distinct value  $|\bar{\sigma}_i\rangle$  is measured.
- 6:      $S = S + 1$
- 7: **end while**
- 8: For each distinct  $\bar{\sigma}_i$  measured, output  $\bar{\sigma}_i$  and its factor score  $\bar{\lambda}_i = \bar{\sigma}_i^2$ .
- 9: For each distinct  $\bar{\sigma}_i$  measured, output its factor score ratio  $\bar{\lambda}^{(i)} = \frac{\zeta_{\bar{\sigma}_i}}{S}$ , where  $\zeta_{\bar{\sigma}_i}$  is the number of times  $|\bar{\sigma}_i\rangle$  has been observed among the measurements. Each estimate comes with confidence level  $z$ .

---

**Theorem 8: Quantum factor score ratio estimation**

**Theorem** (Quantum factor score ratio estimation). *Let there be efficient quantum access to a matrix  $\mathbf{A} \in \mathbb{R}^{n \times m}$ , with singular value decomposition  $\mathbf{A} = \sum_i \sigma_i \mathbf{u}_i \mathbf{v}_i^T$  and  $\sigma_{\max} \leq 1$ . Let  $\gamma, \epsilon$  be precision parameters. There exists a quantum algorithm that, in time  $\tilde{O}\left(\frac{1}{\gamma^2} \frac{\mu(\mathbf{A})}{\epsilon}\right)$ , estimates:*

- the factor score ratios  $\lambda^{(i)}$ , such that  $\|\lambda^{(i)} - \bar{\lambda}^{(i)}\| \leq \gamma$ , with high probability;
- the correspondent singular values  $\sigma_i$ , such that  $\|\sigma_i - \bar{\sigma}_i\| \leq \epsilon$ , with probability at least  $1 - 1/\text{poly}(n)$ ;
- the correspondent factor scores  $\lambda_i$ , such that  $\|\lambda_i - \bar{\lambda}_i\| \leq 2\epsilon$ , with probability at least  $1 - 1/\text{poly}(n)$ .

The proof consists in proving the time complexity and error of Algorithm 1.

*Proof.* As a consequence of Definition 1, the cost of step 3 is  $\tilde{O}(1)$ . The singular value estimation in step 4 can be performed, using Theorem 3, in time  $\tilde{O}\left(\frac{\mu(\mathbf{A})}{\tau}\right)$ , such that  $\|\sigma_i - \bar{\sigma}_i\| \leq \tau$  with probability at least  $1 - 1/\text{poly}(n)$ . A measurement of the third register of the state at step 5 can output any  $\bar{\sigma}_i$  with probability  $\lambda^{(i)} = \frac{\sigma_i^2}{\sum_j^r \sigma_j^2}$ . The total cost of the loop body is  $\tilde{O}\left(\frac{\mu(\mathbf{A})}{\tau}\right)$ . To evaluate the number measurements needed, we can model the measurement process as performing  $r$  Bernoulli trials: one for each  $\bar{\lambda}^{(i)}$ , so that if we measure  $\bar{\sigma}_i$  it is a success for the  $i^{\text{th}}$  Bernoulli trial and a failure for all the others. We use the estimator  $\bar{\lambda}^{(i)} = \frac{\zeta_{\bar{\sigma}_i}}{S}$ , where  $\zeta_{\bar{\sigma}_i}$  is the number of times  $\bar{\sigma}_i$  appears in the measurements and  $S$  is the number of total measurements. Given a confidence level  $z$  and an absolute error  $\gamma$ , it is possible to use the Wald confidence interval to determine a value for  $S$  such that  $\|\lambda^{(i)} - \bar{\lambda}^{(i)}\| \leq \gamma$  with confidence level  $z$ . It is possible to show that  $\gamma \leq \frac{z}{2\sqrt{S}}$  [52], from which we get  $S = \frac{z^2}{4\gamma^2}$ . Since  $z$  is a small number, we can state that the complexity of the algorithm is  $\tilde{O}\left(\frac{1}{\gamma^2} \frac{\mu(\mathbf{A})}{\tau}\right)$ .

We now need to discuss the error of  $\sigma_i$  and  $\lambda_i$ . If we run the algorithm to estimate the singular values  $\sigma_i$  then trivially  $\tau = \epsilon$  and the complexity of the algorithm is  $\tilde{O}\left(\frac{1}{\gamma^2} \frac{\mu(\mathbf{A})}{\epsilon}\right)$ . On the other hand, if the goal is to estimate  $\lambda_i = \sigma_i^2$ , we need to prove that  $\tau \sim \epsilon$ . Running the SVE with precision  $\tau$  means that for each singular value  $\sigma_i$ , with probability  $1 - 1/\text{poly}(n)$ , we have an estimate  $\bar{\sigma}_i$  that in the worst case is  $\bar{\sigma}_i = \sigma_i \pm \tau$ . It follows that

the worst estimate of  $\lambda_i$  is  $\bar{\sigma}_i^2 = (\sigma_i \pm \tau)^2 = \sigma_i^2 \pm 2\sigma_i\tau + \tau^2$  and since  $0 \leq \sigma_i \leq 1$ , we can say that in the worst case  $\bar{\sigma}_i^2 = \sigma_i^2 + (2\tau + \tau^2)$ . Solving the equation  $2\tau + \tau^2 = \epsilon$  for  $\tau > 0$  leads to  $\tau = \sqrt{1 + \epsilon} - 1$ .

$$\tau = \sqrt{1 + \epsilon} - 1 = \frac{(\sqrt{1 + \epsilon} - 1)(\sqrt{1 + \epsilon} + 1)}{(\sqrt{1 + \epsilon} + 1)} = \frac{1 + \epsilon - 1}{\sqrt{1 + \epsilon} + 1} = \frac{\epsilon}{\sqrt{1 + \epsilon} + 1} \sim \frac{\epsilon}{2}. \quad (1)$$

The algorithm can be run  $\tilde{O}\left(\frac{1}{\gamma^2} \frac{\mu(\mathbf{A})}{\epsilon}\right)$  times in both cases and the error on the factor scores cannot be more than the double of the error on the singular values.  $\square$

One limitation of Algorithm 1 is that the Wald confidence interval is not a simultaneous confidence interval. For this reason, it is not guaranteed that all the factor score ratios estimates are computed with precision  $\gamma$  with the same confidence. We have stated the proof using the Wald confidence interval for the sake of simplicity and because we believe that it provides good estimates in practice. To overcome this problem it is possible to adjust the confidence level according to the number of estimated factor scores (e.g. with a Bonferroni correction) or to slightly modify the algorithm to use  $\ell_\infty$  state-vector tomography (Theorem 7) on the state in Step 4. The modified version of the algorithm still has an asymptotic run-time of  $\tilde{O}\left(\frac{1}{\gamma^2} \frac{\mu(\mathbf{A})}{\epsilon}\right)$ , while providing that all  $\|\lambda^{(i)} - \bar{\lambda}^{(i)}\| \leq \gamma$  with probability at least  $1 - 1/\text{poly}(r)$ , where  $r$  is the rank of  $\mathbf{A}$ .

---

**Algorithm 2** Quantum check on the factor score ratios' sum.

---

- 1: Prepare the state  $\frac{1}{\|\mathbf{A}\|_F} \sum_i^n \sum_j^m a_{ij} |i\rangle |j\rangle$ .
- 2: Apply SVE to get  $\frac{1}{\sqrt{\sum_j^r \sigma_j^2}} \sum_i^r \sigma_i |\mathbf{u}_i\rangle |\mathbf{v}_i\rangle |\bar{\sigma}_i\rangle$ .
- 3: Append a quantum register  $|0\rangle$  to the state and set it to  $|1\rangle$  if  $\bar{\sigma}_i < \theta$ .
- 4: Uncompute the SVE  $\frac{1}{\sqrt{\sum_j^r \sigma_j^2}} \sum_{i: \bar{\sigma}_i \geq \theta} \sigma_i |\mathbf{u}_i\rangle |\mathbf{v}_i\rangle |0\rangle + \frac{1}{\sqrt{\sum_j^r \sigma_j^2}} \sum_{i: \bar{\sigma}_i < \theta} \sigma_i |\mathbf{u}_i\rangle |\mathbf{v}_i\rangle |1\rangle$
- 5: Perform amplitude estimation, with precision  $\eta$ , on the last register being  $|0\rangle$ , to estimate  $p = \frac{\sum_{i: \bar{\sigma}_i \geq \theta} \sigma_i^2}{\sum_j^r \sigma_j^2} = \sum_{i: \bar{\sigma}_i \geq \theta} \lambda^{(i)}$ .

---

**Theorem 9: Quantum check on the sum of factor score ratios**

**Theorem** (Quantum check on the factor score ratios' sum). *Let there be efficient quantum access to the matrix  $\mathbf{A} \in \mathbb{R}^{n \times m}$ , with singular value decomposition  $\mathbf{A} = \sum_i \sigma_i \mathbf{u}_i \mathbf{v}_i^T$ . Let  $\eta, \epsilon$  be precision parameters and  $\theta$  be a threshold for the smallest singular value to consider. There exists a quantum algorithm that estimates  $p = \frac{\sum_{i: \bar{\sigma}_i \geq \theta} \sigma_i^2}{\sum_j^r \sigma_j^2}$ , where  $\|\sigma_i - \bar{\sigma}_i\| \leq \epsilon$ , to relative error  $\eta$  in time  $\tilde{O}\left(\frac{\mu(\mathbf{A})}{\epsilon} \frac{1}{\eta \sqrt{p}}\right)$ .*

The proof consists in proving the time complexity of Algorithm 2.

*Proof.* Using Definition 1, step 1 is  $\tilde{O}(1)$ . Singular value estimation in step 2 can be performed using Theorem 3 in time  $\tilde{O}\left(\frac{\mu(\mathbf{A})}{\epsilon}\right)$ . The complexity of step 3 is  $\tilde{O}(1)$  as it is an arithmetic operation that only depends on the binary encoding of  $|\bar{\sigma}_i\rangle$ . Step 4 consists in uncomputing step 2 and has its same cost. The cost so far (step 4) is  $T(U_4) = \tilde{O}\left(\frac{\mu(\mathbf{A})}{\epsilon}\right)$ . Finally, the cost of amplitude estimation, with relative precision  $\eta$ , on the last register

being  $|0\rangle$  is equal to  $O\left(T(U_4)\frac{1}{\eta\sqrt{p}}\right)$ , where  $p = \frac{\sum_{i:\bar{\sigma}_i \geq \theta} \sigma_i^2}{\sum_j \sigma_j^2}$  is the probability of measuring  $|0\rangle$  (Theorem 5). The overall complexity is proven:  $\tilde{O}\left(\frac{\mu(\mathbf{A})}{\epsilon} \frac{1}{\eta\sqrt{p}}\right)$ .  $\square$

---

**Algorithm 3** Quantum top-k singular vectors extraction.

---

- 1: Prepare the state  $\frac{1}{\|\mathbf{A}\|_F} \sum_i^n \sum_j^m a_{ij} |i\rangle |j\rangle$ .
- 2: Apply SVE to get  $\frac{1}{\sqrt{\sum_j^r \sigma_j^2}} \sum_i^r \sigma_i |\mathbf{u}_i\rangle |\mathbf{v}_i\rangle |\bar{\sigma}_i\rangle$ .
- 3: Append a quantum register  $|0\rangle$  to the state and set it to  $|1\rangle$  if  $|\bar{\sigma}_i\rangle < \theta$ .
- 4: Perform amplitude amplification for  $|0\rangle$ , to get the state  $\frac{1}{\sqrt{\sum_j^k \sigma_j^2}} \sum_i^k \sigma_i |\mathbf{u}_i\rangle |\mathbf{v}_i\rangle |\bar{\sigma}_i\rangle$ .
- 5: Append a second ancillary register  $|0\rangle$  and perform the controlled rotation  $\frac{C}{\|\mathbf{A}^{(k)}\|_F} \sum_i^k \frac{\sigma_i}{\bar{\sigma}_i} |\mathbf{u}_i\rangle |\mathbf{v}_i\rangle |\bar{\sigma}_i\rangle |0\rangle + \frac{1}{\|\mathbf{A}^{(k)}\|_F} \sum_i^k \sqrt{1 - \frac{C^2}{\bar{\sigma}_i^2}} |\mathbf{u}_i\rangle |\mathbf{v}_i\rangle |\bar{\sigma}_i\rangle |1\rangle$ , where  $C$  is a normalization constant.
- 6: Perform again amplitude amplification for  $|0\rangle$  to get  $\frac{1}{\sqrt{k}} \sum_i^k |\mathbf{u}_i\rangle |\mathbf{v}_i\rangle |\bar{\sigma}_i\rangle$ .
- 7: Measure the last register and, according to the measured  $|\bar{\sigma}_i\rangle$ , apply state-vector tomography on  $|\mathbf{u}_i\rangle$  for the  $i^{th}$  left singular vector or on  $|\mathbf{v}_i\rangle$  for the right one.
- 8: Repeat 1-7 until the tomography requirements are met.
- 9: Output the  $k$  singular vectors  $\mathbf{u}_i$  or  $\mathbf{v}_i$  and, optionally, the singular values  $\bar{\sigma}_i$ .

---

**Theorem 11, Corollary 12: Quantum top-k singular vectors extraction**

**Theorem** (Top-k singular vectors extraction). *Let there be efficient quantum access to the matrix  $\mathbf{A} \in \mathbb{R}^{n \times m}$ , with singular value decomposition  $\mathbf{A} = \sum_i^r \sigma_i \mathbf{u}_i \mathbf{v}_i^T$  and  $\sigma_{\max} \leq 1$ . Let  $\delta > 0$  be a precision parameter for the singular vectors,  $\epsilon > 0$  a precision parameter for the singular values, and  $\theta > 0$  be a threshold such that  $\mathbf{A}$  has  $k$  singular values greater than  $\theta$ . Define  $p = \frac{\sum_{i:\bar{\sigma}_i \geq \theta} \sigma_i^2}{\sum_j \sigma_j^2}$ . There exist quantum algorithms that estimate:*

- The top  $k$  left singular vectors  $\mathbf{u}_i$  of  $\mathbf{A}$  with unit vectors  $\bar{\mathbf{u}}_i$  such that  $\|\mathbf{u}_i - \bar{\mathbf{u}}_i\|_2 \leq \delta$  with probability at least  $1 - 1/\text{poly}(n)$ , in time  $\tilde{O}\left(\frac{1}{\theta} \frac{1}{\sqrt{p}} \frac{\mu(\mathbf{A})}{\epsilon} \frac{kn}{\delta^2}\right)$ ;
- The top  $k$  right singular vectors  $\mathbf{v}_i$  of  $\mathbf{A}$  with unit vectors  $\bar{\mathbf{v}}_i$  such that  $\|\mathbf{v}_i - \bar{\mathbf{v}}_i\|_2 \leq \delta$  with probability at least  $1 - 1/\text{poly}(m)$ , in time  $\tilde{O}\left(\frac{1}{\theta} \frac{1}{\sqrt{p}} \frac{\mu(\mathbf{A})}{\epsilon} \frac{km}{\delta^2}\right)$ .
- The top  $k$  singular values  $\sigma_i$  and factor scores  $\lambda_i$  of  $\mathbf{A}$  to precision  $\epsilon$  and  $2\epsilon$  with probability at least  $1 - 1/\text{poly}(m)$ , in time  $\tilde{O}\left(\frac{1}{\theta} \frac{1}{\sqrt{p}} \frac{\mu(\mathbf{A})k}{\epsilon}\right)$  or any of the two above.

**Corollary** (Fast top-k singular vectors extraction). *The run-times of 11 can be improved to  $\tilde{O}\left(\frac{1}{\theta} \frac{1}{\sqrt{p}} \frac{\mu(\mathbf{A})}{\epsilon} \frac{k}{\delta^2}\right)$  with estimation guarantees on the  $\ell_\infty$  norms.*

The proof consists in proving the time complexity and the error of Algorithm 3.

*Proof.* As a consequence of Definition 1, step 1 is  $\tilde{O}(1)$ . Singular value estimation in step 2 can be performed using Theorem 3 in time  $\tilde{O}\left(\frac{\mu(\mathbf{A})}{\epsilon}\right)$ . The complexity of step 3 is  $\tilde{O}(1)$ , as it is an arithmetic operation that only depends on the binary encoding of  $|\bar{\sigma}_i\rangle$ . The cost of obtaining the quantum state at step 3 is  $T(U_3) = \tilde{O}\left(\frac{\mu(\mathbf{A})}{\epsilon}\right)$  and the probability of measuring  $|0\rangle$  in the last register is  $p = \frac{\sum_{i:\bar{\sigma}_i \geq \theta} \sigma_i^2}{\sum_j \sigma_j^2}$ : the complexity of amplitude amplification at step 4, using Theorem 5, is  $\tilde{O}\left(\frac{1}{\sqrt{p}} \frac{\mu(\mathbf{A})}{\epsilon}\right)$ . Step 5 consists in a conditional rotation and similarly

to step 3 it has a negligible cost. The next step is to analyze the amplitude amplification at 6. We have the state  $\frac{C}{\|\mathbf{A}^{(k)}\|_F} \sum_i^k \frac{\sigma_i}{\bar{\sigma}_i} |\mathbf{u}_i\rangle |\mathbf{v}_i\rangle |\bar{\sigma}_i\rangle |0\rangle + \frac{1}{\|\mathbf{A}^{(k)}\|_F} \sum_i^k \sqrt{1 - \frac{C^2}{\bar{\sigma}_i^2}} |\mathbf{u}_i\rangle |\mathbf{v}_i\rangle |\bar{\sigma}_i\rangle |1\rangle$ .

The constant  $C$  is a normalization factor in the order of  $\tilde{O}(1/\kappa(\mathbf{A}^{(k)}))$  where  $\kappa(\mathbf{A}^{(k)}) = \frac{\sigma_{\max}}{\sigma_{\min}}$  is the condition number of the low-rank matrix  $\mathbf{A}^{(k)}$ . Since for construction  $\sigma_{\max} \leq 1$  and  $\sigma_{\min} \geq \theta$ , we can bound the condition number  $\kappa(\mathbf{A}^{(k)}) \leq \frac{1}{\theta}$ . From the famous work of Harrow, Hassidim and Lloyd [23] we know that applying amplitude amplification on the state above, with the the third register being  $|0\rangle$ , would cost  $\tilde{O}(\kappa(\mathbf{A}^{(k)})T(U_5))$ .

In our case, the cost of step 6 is  $\tilde{O}\left(\frac{1}{\theta} \frac{1}{\sqrt{p}} \frac{\mu(\mathbf{A})}{\epsilon}\right)$ , and amplitude amplification leaves the registers in the state

$$\frac{1}{\sqrt{\sum_i^k \frac{\sigma_i^2}{\bar{\sigma}_i^2}}} \sum_i^k \frac{\sigma_i}{\bar{\sigma}_i} |\mathbf{u}_i\rangle |\mathbf{v}_i\rangle |\bar{\sigma}_i\rangle \sim \frac{1}{\sqrt{k}} \sum_i^k |\mathbf{u}_i\rangle |\mathbf{v}_i\rangle |\bar{\sigma}_i\rangle \quad (2)$$

where  $\bar{\sigma}_i \in [\sigma_i - \epsilon, \sigma_i + \epsilon]$  and  $\frac{\sigma_i}{\sigma_i \pm \epsilon} \rightarrow 1$  for  $\epsilon \rightarrow 0$ .

The last step of the proof is to compute the time complexity of the state-vector tomography at step 7. When measuring the last register of state 6 in the computational basis and obtaining  $|\bar{\sigma}_i\rangle$ , the first two registers collapse in the state  $|\mathbf{u}_i\rangle |\mathbf{v}_i\rangle$ . On  $|\mathbf{u}_i\rangle |\mathbf{v}_i\rangle$ , it is possible to perform vector-state tomography using Theorem 6 either on the first register, to retrieve  $\bar{\mathbf{u}}_i$ , or on the second one, to retrieve  $\bar{\mathbf{v}}_i$ . Since  $\mathbf{u}_i \in \mathbb{R}^n$  and  $\mathbf{v}_i \in \mathbb{R}^m$ , performing state-vector tomography on the first register takes time  $O(\frac{n \log n}{\delta^2})$  and performing it on the second takes time  $O(\frac{m \log m}{\delta^2})$ . Using a coupon collector's argument [13], if the  $k$  states  $|\bar{\sigma}_i\rangle$  are uniformly distributed, to get all the  $k$  possible couples  $|\mathbf{u}_i\rangle |\mathbf{v}_i\rangle$  at least once we would need  $k \log k$  measurements on average. This proves that it is possible to estimate all the singular values, with the guarantees of Theorem 3 in time  $\tilde{O}(\frac{1}{\theta} \frac{1}{\sqrt{p}} \frac{\mu(\mathbf{A})k}{\epsilon})$ . To perform tomography on each state-vector, one should satisfy the coupon collector the same number of times as the measurements needed by the tomography procedure. The costs of the tomography for all the vectors  $\{\bar{\mathbf{u}}_i\}_i^k$  and  $\{\bar{\mathbf{v}}_i\}_i^k$  are  $O\left(T(U_6) \frac{k \log k \cdot n \log n}{\delta^2}\right)$ , and  $O\left(T(U_6) \frac{k \log k \cdot m \log m}{\delta^2}\right)$ . Therefore, the following complexities are proven:  $\tilde{O}\left(\frac{1}{\theta} \frac{1}{\sqrt{p}} \frac{\mu(\mathbf{A})}{\epsilon} \frac{kn}{\delta^2}\right)$ ,  $\tilde{O}\left(\frac{1}{\theta} \frac{1}{\sqrt{p}} \frac{\mu(\mathbf{A})}{\epsilon} \frac{km}{\delta^2}\right)$ .

The proof for Corollary 12 consists in using Theorem 7 to perform the tomography at step 7.  $\square$

In Section C.2, we provide experiments that show that the coupon collector's prediction of Eq. 2 is accurate for practical  $\epsilon$ .

### Lemma 13: Accuracy of $\bar{\mathbf{U}}\bar{\Sigma}$ and $\bar{\mathbf{V}}\bar{\Sigma}$

**Lemma** (Accuracy of  $\bar{\mathbf{U}}\bar{\Sigma}$  and  $\bar{\mathbf{V}}\bar{\Sigma}$ ). *Let  $\mathbf{A} \in \mathbb{R}^{n \times m}$  be a matrix with  $\sigma_{\max} \leq 1$ . Given some approximate procedures to retrieve estimates  $\bar{\sigma}_i$  of the singular values  $\sigma_i$  such that  $\|\sigma_i - \bar{\sigma}_i\| \leq \epsilon$  and unit estimates  $\bar{\mathbf{u}}_i$  of the left singular vectors  $\mathbf{u}_i$  such that  $\|\bar{\mathbf{u}}_i - \mathbf{u}_i\|_2 \leq \delta$ , the error on  $\bar{\mathbf{U}}\bar{\Sigma}$  can be bounded as  $\|\mathbf{U}\Sigma - \bar{\mathbf{U}}\bar{\Sigma}\|_F \leq \sqrt{k}(\epsilon + \delta)$ . Similarly,  $\|\mathbf{V}\Sigma - \bar{\mathbf{V}}\bar{\Sigma}\|_F \leq \sqrt{k}(\epsilon + \delta)$ .*

We prove this result for  $\|\mathbf{U}\Sigma - \bar{\mathbf{U}}\bar{\Sigma}\|_F$ , the prof for  $\|\mathbf{V}\Sigma - \bar{\mathbf{V}}\bar{\Sigma}\|_F$  proceeds analogously.

*Proof.* The first step of the proof consists in bounding the error on the columns of the matrices:  $\|\bar{\sigma}_i \bar{\mathbf{u}}_i - \sigma_i \mathbf{u}_i\|$ .

$$\|\bar{\sigma}_i \bar{\mathbf{u}}_i - \sigma_i \mathbf{u}_i\| \leq \|(\sigma_i \pm \epsilon) \bar{\mathbf{u}}_i - \sigma_i \mathbf{u}_i\| = \|\sigma_i(\bar{\mathbf{u}}_i - \mathbf{u}_i) \pm \epsilon \bar{\mathbf{u}}_i\| \quad (3)$$

Because of the triangular inequality,  $\|\sigma_i(\bar{\mathbf{u}}_i - \mathbf{u}_i) \pm \epsilon \bar{\mathbf{u}}_i\| \leq \sigma_i \|\bar{\mathbf{u}}_i - \mathbf{u}_i\| + \epsilon \|\bar{\mathbf{u}}_i\|$ . Also by hypothesis,  $\|(\bar{\mathbf{u}}_i - \mathbf{u}_i)\| \leq \delta$  and  $\|\bar{\mathbf{u}}_i\| = 1$ . Thus,  $\sigma_i \|\bar{\mathbf{u}}_i - \mathbf{u}_i\| + \epsilon \|\bar{\mathbf{u}}_i\| \leq \sigma_i \delta + \epsilon$ . From the error bound on the columns and the fact that  $f(x) = \sqrt{x}$  is an increasing monotone function, it is possible to prove the error bound on the matrices:

$$\begin{aligned} \|\bar{\mathbf{U}}\bar{\Sigma} - \mathbf{U}\Sigma\|_F &= \sqrt{\sum_i^n \sum_j^k \|\bar{\sigma}_j \bar{u}_{ij} - \sigma_j u_{ij}\|^2} = \sqrt{\sum_j^k (\|\bar{\sigma}_j \bar{\mathbf{u}}_j - \sigma_j \mathbf{u}_j\|)^2} \\ &\leq \sqrt{\sum_j^k (\epsilon + \delta \sigma_j)^2} \leq \sqrt{k(\epsilon + \delta \sigma_{max})^2} \leq \sqrt{k}(\epsilon + \delta \|\mathbf{A}\|) \end{aligned} \quad (4)$$

Finally, since  $\sigma_{max} \leq 1$ , we get that  $\|\bar{\mathbf{U}}\bar{\Sigma} - \mathbf{U}\Sigma\|_F \leq \sqrt{k}(\epsilon + \delta)$ .  $\square$

### Lemma 20: Accuracy of $D_X^{-1/2}\bar{\mathbf{U}}$ and $D_Y^{-1/2}\bar{\mathbf{U}}$

**Lemma** (Accuracy of  $D_X^{-1/2}\mathbf{U}$  and  $D_Y^{-1/2}\mathbf{V}$ ). *Let  $\mathbf{A} \in \mathbb{R}^{n \times m}$  be a matrix. Given some approximate procedures to retrieve unit estimates  $\bar{\mathbf{u}}_i$  of the left singular vectors  $\mathbf{u}_i$  such that  $\|\bar{\mathbf{u}}_i - \mathbf{u}_i\| \leq \delta$ , the error on  $D_X^{-1/2}\mathbf{U}$  can be bounded as  $\|D_X^{-1/2}\mathbf{U} - D_X^{-1/2}\bar{\mathbf{U}}\|_F \leq \|D_X^{-1/2}\|_F \sqrt{k} \delta$ . Similarly,  $\|D_Y^{-1/2}\mathbf{V} - D_Y^{-1/2}\bar{\mathbf{V}}\|_F \leq \|D_Y^{-1/2}\|_F \sqrt{k} \delta$ .*

We prove this result for  $\|D_X^{-1/2}\bar{\mathbf{U}} - D_X^{-1/2}\mathbf{U}\|_F$ .

*Proof.*

$$\|D_X^{-1/2}\bar{\mathbf{U}} - D_X^{-1/2}\mathbf{U}\|_F \leq \|D_X^{-1/2}\|_F \|\bar{\mathbf{U}} - \mathbf{U}\|_F \leq \|D_X^{-1/2}\|_F \sqrt{k} \delta \quad (5)$$

$\square$

### Lemma 21: Accuracy of $\bar{\mathbf{U}}\bar{\Sigma}^{1/2}$ and $\bar{\mathbf{V}}\bar{\Sigma}^{1/2}$

**Lemma** (Accuracy of  $\bar{\mathbf{U}}\bar{\Sigma}^{1/2}$  and  $\bar{\mathbf{V}}\bar{\Sigma}^{1/2}$ ). *Let  $\mathbf{A} \in \mathbb{R}^{n \times m}$  be a matrix with  $\sigma_{max} \leq 1$ . Given some approximate procedures to retrieve estimates  $\bar{\sigma}_i$  of the singular values  $\sigma_i$  such that  $\|\bar{\sigma}_i - \sigma_i\| \leq \epsilon$  and unitary estimates  $\bar{\mathbf{u}}_i$  of the left singular vectors  $\mathbf{u}_i$  such that  $\|\bar{\mathbf{u}}_i - \mathbf{u}_i\| \leq \delta$ , the error on  $\mathbf{U}\Sigma^{1/2}$  can be bounded as  $\|\mathbf{U}\Sigma^{1/2} - \bar{\mathbf{U}}\bar{\Sigma}^{1/2}\|_F \leq \sqrt{k} \left( \delta + \frac{1}{2\sqrt{\theta}} \right)$ . Similarly,  $\|\mathbf{V}\Sigma^{1/2} - \bar{\mathbf{V}}\bar{\Sigma}^{1/2}\|_F \leq \sqrt{k} \left( \delta + \frac{1}{2\sqrt{\theta}} \right)$ .*

We prove this result for  $\|\bar{\mathbf{U}}\bar{\Sigma}^{1/2} - \mathbf{U}\Sigma^{1/2}\|_F$ .

*Proof.* We start by bounding  $\|\sqrt{\bar{\sigma}_i} - \sqrt{\sigma_i}\|$ . Let's define  $\epsilon = \gamma \sigma_i$  as a relative error:

$$\begin{aligned} \|\sqrt{\sigma_i + \epsilon} - \sqrt{\sigma_i}\| &= \|\sqrt{\sigma_i + \gamma \sigma_i} - \sqrt{\sigma_i}\| = \|\sqrt{\sigma_i}(\sqrt{1 + \gamma} - 1)\| \\ &= \sqrt{\sigma_i} \left\| \frac{(\sqrt{1 + \gamma} - 1)(\sqrt{1 + \gamma} + 1)}{\sqrt{1 + \gamma} + 1} \right\| \end{aligned} \quad (6)$$

$$= \sqrt{\sigma_i} \left\| \frac{\gamma + 1 - 1}{\sqrt{1 + \gamma} + 1} \right\| \leq \sqrt{\sigma_i} \frac{\gamma}{2}. \quad (7)$$

By definition  $\gamma = \frac{\epsilon}{\sigma_i}$  and we know that  $\sigma_{min} \geq \theta$ :

$$\|\sqrt{\sigma_i} - \sqrt{\sigma_i}\| \leq \frac{\sqrt{\sigma_i} \epsilon}{\sigma_1} \frac{\epsilon}{2} = \frac{\epsilon}{2\sqrt{\sigma_i}} \leq \frac{\epsilon}{2\sqrt{\theta}}. \quad (8)$$

Using the bound on the square roots, we can bound the columns of  $\bar{\mathbf{U}}\bar{\Sigma}^{1/2}$ :

$$\begin{aligned} \left\| \sqrt{\sigma_i} \bar{\mathbf{u}}_i - \sqrt{\sigma_i} \mathbf{u}_i \right\| &\leq \left\| \left( \sqrt{\sigma_i} + \frac{\epsilon}{2\sqrt{\theta}} \right) \bar{\mathbf{u}}_i - \sqrt{\sigma_i} \mathbf{u}_i \right\| = \\ \left\| \sqrt{\sigma_i} (\bar{\mathbf{u}}_i - \mathbf{u}_i) + \frac{\epsilon}{2\sqrt{\theta}} \bar{\mathbf{u}}_i \right\| &\leq \sqrt{\sigma_i} \delta + \frac{\epsilon}{2\sqrt{\theta}} \leq \delta \sqrt{\|\mathbf{A}\|} + \frac{\epsilon}{2\sqrt{\theta}}. \end{aligned} \quad (9)$$

From the error bound on the columns we derive the bound on the matrices:

$$\left\| \bar{\mathbf{U}}\bar{\Sigma}^{1/2} - \mathbf{U}\Sigma^{1/2} \right\|_F = \sqrt{\sum_j^k (\|\sqrt{\sigma_j} \bar{\mathbf{u}}_j - \sqrt{\sigma_j} \mathbf{u}_j\|)^2} \leq \sqrt{k} \left( \delta \sqrt{\|\mathbf{A}\|} + \frac{\epsilon}{2\sqrt{\theta}} \right). \quad (10)$$

Finally, since  $\sigma_{max} \leq 1$ , we get that  $\|\bar{\mathbf{U}}\bar{\Sigma}^{1/2} - \mathbf{U}\Sigma^{1/2}\|_F \leq \sqrt{k}(\delta + \frac{\epsilon}{2\sqrt{\theta}})$ .  $\square$

### Lemma 22: Accuracy of $\bar{\mathbf{U}}\bar{\Sigma}^{-1}$ and $\bar{\mathbf{V}}\bar{\Sigma}^{-1}$

**Lemma** (Accuracy of  $\bar{\mathbf{U}}\bar{\Sigma}^{-1}$  and  $\bar{\mathbf{V}}\bar{\Sigma}^{-1}$ ). *Let  $\mathbf{A} \in \mathbb{R}^{n \times m}$  be a matrix. Given some approximate procedures to retrieve estimates  $\bar{\sigma}_i$  of the singular values  $\sigma_i$  such that  $|\bar{\sigma}_i - \sigma_i| \leq \epsilon$  and unitary estimates  $\bar{\mathbf{u}}_i$  of the left singular vectors  $\mathbf{u}_i$  such that  $\|\bar{\mathbf{u}}_i - \mathbf{u}_i\| \leq \delta$ , the error on  $\mathbf{U}\Sigma^{-1}$  can be bounded as  $\|\mathbf{U}\Sigma^{-1} - \bar{\mathbf{U}}\bar{\Sigma}^{-1}\|_F \leq \sqrt{k} \left( \frac{\delta}{\theta} + \frac{\epsilon}{\theta^2 - \theta\epsilon} \right)$ . Similarly,  $\|\mathbf{V}\Sigma^{-1} - \bar{\mathbf{V}}\bar{\Sigma}^{-1}\|_F \leq \sqrt{k} \left( \frac{\delta}{\theta} + \frac{\epsilon}{\theta^2 - \theta\epsilon} \right)$ .*

We prove this result for  $\|\bar{\mathbf{U}}\bar{\Sigma}^{-1} - \mathbf{U}\Sigma^{-1}\|_F$ .

*Proof.* We start by bounding  $\left\| \frac{1}{\bar{\sigma}_i} - \frac{1}{\sigma_i} \right\|$ , knowing that  $\sigma_{min} \geq \theta$  and  $\epsilon < \theta$ :

$$\left\| \frac{1}{\bar{\sigma}_i} - \frac{1}{\sigma_i} \right\| \leq \left\| \frac{1}{\sigma_i - \epsilon} - \frac{1}{\sigma_i} \right\| \leq \frac{\epsilon}{\theta^2 - \theta\epsilon}. \quad (11)$$

From the bound on the inverses, we can obtain the bound on the columns of  $\bar{\mathbf{U}}\bar{\Sigma}^{-1}$ :

$$\left\| \frac{1}{\bar{\sigma}_i} \bar{\mathbf{u}}_i - \frac{1}{\sigma_i} \mathbf{u}_i \right\| \leq \left\| \left( \frac{1}{\sigma_i} \pm \frac{\epsilon}{\theta^2 - \theta\epsilon} \right) \bar{\mathbf{u}}_i - \frac{1}{\sigma_i} \mathbf{u}_i \right\| \leq \frac{1}{\sigma_i} \delta + \frac{\epsilon}{\theta^2 - \theta\epsilon} \leq \frac{\delta}{\theta} + \frac{\epsilon}{\theta^2 - \theta\epsilon}. \quad (12)$$

To end the proof, we can compute the bound on the matrices:

$$\left\| \bar{\mathbf{U}}\bar{\Sigma}^{-1} - \mathbf{U}\Sigma^{-1} \right\|_F = \sqrt{\sum_j^k \left( \left\| \frac{1}{\bar{\sigma}_j} \bar{\mathbf{u}}_j - \frac{1}{\sigma_j} \mathbf{u}_j \right\| \right)^2} \leq \sqrt{k} \left( \frac{\delta}{\theta} + \frac{\epsilon}{\theta^2 - \theta\epsilon} \right) \quad (13)$$

$\square$

**Claim 14, 23, 24: Not-normalized accuracy**

**Claim** (Non-normalized  $\bar{\mathbf{U}}\Sigma$  and  $\bar{\mathbf{V}}\Sigma$ ). *The estimated representations of Lemma 13, for the not-normalized matrix  $\mathbf{A}$ , are  $\|\mathbf{A}\|\bar{\mathbf{U}}\Sigma$  and  $\|\mathbf{A}\|\bar{\mathbf{V}}\Sigma$ . The error bounds become  $\left\| \|\mathbf{A}\|\mathbf{U}\Sigma - \|\mathbf{A}\|\bar{\mathbf{U}}\Sigma \right\|_F \leq \sqrt{k}\|\mathbf{A}\|(\epsilon + \delta)$  and  $\left\| \|\mathbf{A}\|\mathbf{V}\Sigma - \|\mathbf{A}\|\bar{\mathbf{V}}\Sigma \right\|_F \leq \sqrt{k}\|\mathbf{A}\|(\epsilon + \delta)$ .*

**Claim** (Non-normalized  $\bar{\mathbf{U}}\Sigma^{1/2}$  and  $\bar{\mathbf{V}}\Sigma^{1/2}$ ). *The estimated representations of Lemma 21, for the not-normalized matrix  $\mathbf{A}$ , are  $\sqrt{\|\mathbf{A}\|}\bar{\mathbf{U}}\Sigma^{1/2}$  and  $\sqrt{\|\mathbf{A}\|}\bar{\mathbf{V}}\Sigma^{1/2}$ . The error bounds become  $\left\| \sqrt{\|\mathbf{A}\|}\bar{\mathbf{U}}\Sigma^{1/2} - \sqrt{\|\mathbf{A}\|}\mathbf{U}\Sigma^{1/2} \right\|_F \leq \sqrt{k}\|\mathbf{A}\|(\epsilon + \delta)$  and  $\left\| \sqrt{\|\mathbf{A}\|}\bar{\mathbf{V}}\Sigma^{1/2} - \sqrt{\|\mathbf{A}\|}\mathbf{V}\Sigma^{1/2} \right\|_F \leq \sqrt{k}\|\mathbf{A}\|(\epsilon + \delta)$ .*

**Claim** (Non-normalized  $\bar{\mathbf{U}}\Sigma^{-1}$  and  $\bar{\mathbf{V}}\Sigma^{-1}$ ). *The estimated representations of Lemma 22, for the not-normalized matrix  $\mathbf{A}$ , are  $\frac{1}{\|\mathbf{A}\|}\bar{\mathbf{U}}\Sigma^{-1}$  and  $\frac{1}{\|\mathbf{A}\|}\bar{\mathbf{V}}\Sigma^{-1}$ . The error bounds become  $\left\| \frac{1}{\|\mathbf{A}\|}\bar{\mathbf{U}}\Sigma^{-1} - \frac{1}{\|\mathbf{A}\|}\mathbf{U}\Sigma^{1/2} \right\| \leq \frac{\sqrt{k}}{\|\mathbf{A}\|} \left( \frac{\delta}{\theta} + \frac{\epsilon}{\theta^2 - \theta\epsilon} \right)$  and  $\left\| \frac{1}{\|\mathbf{A}\|}\bar{\mathbf{V}}\Sigma^{-1} - \frac{1}{\|\mathbf{A}\|}\mathbf{V}\Sigma^{1/2} \right\| \leq \frac{\sqrt{k}}{\|\mathbf{A}\|} \left( \frac{\delta}{\theta} + \frac{\epsilon}{\theta^2 - \theta\epsilon} \right)$ .*

We prove the first claim, the other proof can be derived analogously.

*Proof.* Firstly, it is easy to see that to get the desired data representations it suffices to multiply the output matrix by  $\|\mathbf{A}\|$ . Indeed, in our quantum memory, the singular values of the non-normalized matrix are scaled by a factor  $\frac{1}{\|\mathbf{A}\|}$ , while the singular vectors remain the same. To prove the bounds, we can just multiply both sides of the inequalities from Lemma 13 by  $\|\mathbf{A}\|$ , which is a positive quantity:

$$\left\| \|\mathbf{A}\|\bar{\mathbf{U}}\Sigma - \|\mathbf{A}\|\mathbf{U}\Sigma \right\|_F \leq \sqrt{k}\|\mathbf{A}\|(\epsilon + \delta),$$

$$\left\| \|\mathbf{A}\|\bar{\mathbf{V}}\Sigma - \|\mathbf{A}\|\mathbf{V}\Sigma \right\|_F \leq \sqrt{k}\|\mathbf{A}\|(\epsilon + \delta).$$

□

**Corollary 15: Quantum PCA, vector dimensionality reduction**

**Corollary** (Quantum PCA: vector dimensionality reduction). *Let  $\xi$  be a precision parameter. Let there be efficient quantum access to the top  $k$  right singular vectors  $\bar{\mathbf{V}}^{(k)} \in \mathbb{R}^{m \times k}$  of a matrix  $\mathbf{A} = \mathbf{U}\Sigma\mathbf{V}^T \in \mathbb{R}^{n \times m}$ , such that  $\|\mathbf{V}^{(k)} - \bar{\mathbf{V}}^{(k)}\| \leq \frac{\xi}{\sqrt{2}}$ . Given efficient quantum access to a row  $\mathbf{a}_i$  of  $\mathbf{A}$ , the quantum state  $|\bar{\mathbf{y}}_i\rangle = \frac{1}{\|\bar{\mathbf{y}}_i\|} \sum_k \bar{y}_k |i\rangle$ , proportional to its projection onto the PCA space, can be created in time  $\tilde{O}\left(\frac{\|\mathbf{a}_i\|}{\|\bar{\mathbf{y}}_i\|}\right)$  with probability at least  $1 - 1/\text{poly}(m)$  and precision  $\||\mathbf{y}_i\rangle - |\bar{\mathbf{y}}_i\rangle\| \leq \frac{\|\mathbf{a}_i\|}{\|\bar{\mathbf{y}}_i\|} \xi$ . An estimate of  $\|\bar{\mathbf{y}}_i\|$ , to relative error  $\eta$ , can be computed in  $\tilde{O}(1/\eta)$ .*

*Proof.* In the proof we use  $\mathbf{V}$  to denote the matrix  $\mathbf{V}^{(k)} \in \mathbb{R}^{m \times k}$ . Given a vector  $\mathbf{a}_i$ , its projection onto the  $k$ -dimensional PCA space of  $\mathbf{A}$  is  $\mathbf{y}_i^T = \mathbf{a}_i^T \mathbf{V}$ , or equivalently  $\mathbf{y}_i = \mathbf{V}^T \mathbf{a}_i$ . Note that  $\|\mathbf{y}_i\| = \|\mathbf{V}^T \mathbf{a}_i\|$ . It is possible to use Theorem 4 to multiply the quantum state  $|\mathbf{a}_i\rangle$  by  $\mathbf{V}^T$ , appropriately padded with 0s to be a square  $\mathbb{R}^{m \times m}$  matrix. Theorem 4 states that it is possible to create an approximation  $|\bar{\mathbf{y}}_i\rangle$  of the state  $|\mathbf{y}_i\rangle = |\mathbf{V}^T \mathbf{a}_i\rangle$  in time  $\tilde{O}\left(\frac{\mu(\mathbf{V}^T) \log(1/\epsilon)}{\gamma}\right)$  with probability  $1 - 1/\text{poly}(m)$ , such that  $\||\mathbf{y}_i\rangle - |\bar{\mathbf{y}}_i\rangle\| \leq \epsilon$ . Since  $\mathbf{V}$  has rows with unit  $\ell_2$  norm, we can use a result from Kerenidis and Prakash [31, Theorem

IV.1] to prepare efficient quantum access to it with  $\mu(\mathbf{V}^T) = 1$ . Choosing the parameter as  $\gamma = \|\mathbf{V}^T \mathbf{a}_i\| / \|\mathbf{a}_i\|$ , we get a run-time of  $\tilde{O}\left(\frac{\|\mathbf{a}_i\|}{\|\mathbf{y}_i\|} \log(1/\epsilon)\right)$ . We can consider the term  $\log(1/\epsilon)$  to be negligible, as, for instance, an error  $\epsilon = 10^{-17}$  would not be relevant in practice, while accounting for a factor 17 in the run-time. We conclude that the state  $|\mathbf{y}_i\rangle$  can be created in time  $\tilde{O}\left(\frac{\|\mathbf{a}_i\|}{\|\mathbf{y}_i\|}\right)$  with probability  $1 - 1/\text{poly}(m)$  and that its norm can be estimated to relative error  $\eta$  in time  $\tilde{O}\left(\frac{\|\mathbf{a}_i\|}{\|\mathbf{y}_i\|} \frac{1}{\eta}\right)$ .

For what concerns the error, we start by bounding  $\|\mathbf{y}_i - \bar{\mathbf{y}}_i\|$  and use Claim 25 to bound the error on the quantum states. We assume to have estimates  $\bar{\mathbf{v}}_i$  of the columns of  $\mathbf{V}$  such that  $\|\mathbf{v}_i - \bar{\mathbf{v}}_i\| \leq \delta$ .

$$\|\mathbf{V} - \bar{\mathbf{V}}\|_F = \sqrt{\sum_i^n \sum_j^k (v_{ij} - \bar{v}_{ij})^2} \leq \sqrt{k}\delta \quad (14)$$

Considering that  $\|\mathbf{y}_i - \bar{\mathbf{y}}_i\| = \|\mathbf{a}_i^T \mathbf{V}^{(k)} - \mathbf{a}_i^T \bar{\mathbf{V}}^{(k)}\| \leq \|\mathbf{a}_i\| \sqrt{k}\delta$ , we can use Claim 25 to state

$$\|\mathbf{y}_i - \bar{\mathbf{y}}_i\| \leq \frac{\|\mathbf{a}_i\|}{\|\mathbf{y}_i\|} \sqrt{2k}\delta = \frac{\|\mathbf{a}_i\|}{\|\mathbf{y}_i\|} \xi. \quad (15)$$

We can set  $\delta = \frac{\xi}{\sqrt{2k}}$  and require  $\|\mathbf{V} - \bar{\mathbf{V}}\|_F \leq \frac{\xi}{\sqrt{2}}$ .  $\square$

### Corollary 16: Quantum PCA, matrix dimensionality reduction

**Corollary** (Quantum PCA: matrix dimensionality reduction). *Let  $\xi$  be a precision parameter and  $p$  be the amount of variance retained after the dimensionality reduction. Let there be efficient quantum access to  $\mathbf{A} = \mathbf{U}\mathbf{\Sigma}\mathbf{V}^T \in \mathbb{R}^{n \times m}$  and to its top  $k$  right singular vectors  $\bar{\mathbf{V}}^{(k)} \in \mathbb{R}^{m \times k}$ , such that  $\|\mathbf{V}^{(k)} - \bar{\mathbf{V}}^{(k)}\| \leq \frac{\xi\sqrt{p}}{\sqrt{2}}$ . There exists a quantum algorithm that, with probability at least  $1 - 1/\text{poly}(m)$ , creates the state  $|\bar{\mathbf{Y}}\rangle = \frac{1}{\|\bar{\mathbf{Y}}\|_F} \sum_i^n \|\mathbf{y}_{i,\cdot}\| |i\rangle |\mathbf{y}_{i,\cdot}\rangle$ , proportional to the projection of  $\mathbf{A}$  in the PCA subspace, with error  $\||\mathbf{Y}\rangle - |\bar{\mathbf{Y}}\rangle\| \leq \xi$  in time  $\tilde{O}(1/\sqrt{p})$ . An estimate of  $\|\bar{\mathbf{Y}}\|_F$ , to relative error  $\eta$ , can be computed in  $\tilde{O}(\frac{1}{\sqrt{pn}})$ .*

*Proof.* In the proof we use  $\mathbf{V}$  to denote the matrix  $\mathbf{V}^{(k)} \in \mathbb{R}^{m \times k}$ . Using the same reasoning as the proof above and giving a closer look at the proof of Theorem 4 (Lemma 24 [8]), we see that it is possible to create the state  $|0\rangle (\bar{\mathbf{V}}^T |\mathbf{a}_i\rangle) + |0_\perp\rangle$  in time  $\tilde{O}(1)$  and that the term  $\frac{1}{\gamma}$  is introduced to boost the probability of getting the right state. If we apply Theorem 4 without the amplitude amplification step to the superposition of the rows of  $\mathbf{A}$ , we obtain the following mapping in time  $\tilde{O}(1)$ :

$$|\mathbf{A}\rangle = \frac{1}{\|\mathbf{A}\|_F} \sum_i^n \|\mathbf{a}_{i,\cdot}\| |i\rangle |\mathbf{a}_{i,\cdot}\rangle \mapsto \frac{1}{\|\mathbf{A}\|_F} \sum_i^n (\|\mathbf{y}_{i,\cdot}\| |0\rangle |i\rangle |\mathbf{y}_{i,\cdot}\rangle + \|\mathbf{y}_{i,\cdot\perp}\| |0_\perp\rangle), \quad (16)$$

where  $\|\mathbf{y}_{i,\cdot\perp}\|$  are normalization factors. Keeping in mind that  $\|\mathbf{A}\|_F = \sqrt{\sum_i^r \sigma_i^2}$  and  $\|\mathbf{Y}\|_F = \sqrt{\sum_i^n \|\mathbf{y}_{i,\cdot}\|^2} = \sqrt{\sum_i^k \sigma_i^2}$ , we see that the amount of explained variance is  $p = \frac{\sum_i^k \sigma_i^2}{\sum_j^r \sigma_j^2} = \left(\frac{\|\mathbf{Y}\|_F}{\|\mathbf{A}\|_F}\right)^2$ . The probability of obtaining  $|\mathbf{Y}\rangle = \frac{1}{\|\mathbf{Y}\|_F} \sum_i^n \|\mathbf{y}_{i,\cdot}\| |i\rangle |\mathbf{y}_{i,\cdot}\rangle$  is  $p = \frac{\|\mathbf{Y}\|_F^2}{\|\mathbf{A}\|_F^2} = \frac{\sum_i^n \|\mathbf{y}_{i,\cdot}\|^2}{\|\mathbf{A}\|_F^2}$ . We conclude that, using  $\tilde{O}(1/\sqrt{p})$  rounds of amplitude amplification, we obtain  $|\mathbf{Y}\rangle$  with probability  $1 - 1/\text{poly}(m)$  (Theorem 5).

Considering that  $\|\mathbf{Y} - \bar{\mathbf{Y}}\| = \|\mathbf{AV}^{(k)} - \mathbf{AV}^{(k)}\| \leq \|\mathbf{A}\|\sqrt{k}\delta$ , we can use Claim 25 to state

$$\|\langle \mathbf{Y} \rangle - \langle \bar{\mathbf{Y}} \rangle\| \leq \frac{\|\mathbf{A}\|_F}{\|\mathbf{Y}\|_F} \sqrt{2k}\delta = \xi. \quad (17)$$

We can set  $\delta = \frac{\xi}{\sqrt{2k}} \frac{\|\mathbf{Y}\|_F}{\|\mathbf{A}\|_F} = \frac{\xi\sqrt{p}}{\sqrt{2k}}$ , so we require  $\|\mathbf{V} - \bar{\mathbf{V}}\|_F \leq \frac{\xi\sqrt{p}}{\sqrt{2}}$ .  $\square$

### Corollary 17: Quantum PCA, fitting time

**Corollary** (Quantum PCA: fitting time). *Let  $\epsilon$  be a precision parameter and  $p = \frac{\sum_{i:\bar{\sigma}_i \geq \theta} \sigma_i^2}{\sum_j \sigma_j^2}$  the amount of variance to retain, where  $\|\sigma_i - \bar{\sigma}_i\| \leq \epsilon$ . Given efficient quantum access to a matrix  $\mathbf{A} \in \mathbb{R}^{n \times m}$ , the run-time to extract  $\mathbf{V}^{(k)} \in \mathbb{R}^{m \times k}$  for corollaries 15, 16 is  $\tilde{O}\left(\frac{\mu(\mathbf{A})k^2m}{\theta\epsilon\xi^2}\right)$ .*

We state the proof for Corollary 16, as its error is more demanding than the one of Corollary 15. This way, the proof stands for both cases.

*Proof.* The procedure to train the model consists in using Theorem 10 to extract the threshold  $\theta$ , given the amount of variance to retain  $p$ , and to leverage Theorem 11 to extract the  $k$  right singular vectors that compose  $\mathbf{V} \in \mathbb{R}^{m \times k}$ . The run-time of Theorem 10 is smaller than the one of Theorem 11, so we can focus on the last one. From the proof of Corollary 16, we know that to have  $\|\mathbf{V} - \bar{\mathbf{V}}\|_F \leq \frac{\xi\sqrt{p}}{\sqrt{2}}$  we need  $\|\mathbf{v}_i - \bar{\mathbf{v}}_i\| \leq \frac{\xi\sqrt{p}}{\sqrt{2k}}$ . Substituting  $\delta = \frac{\xi\sqrt{p}}{\sqrt{2k}}$  in the run-time of Theorem 11, we get  $\tilde{O}\left(\frac{\mu\mathbf{A}k^2m}{p^{3/2}\theta\epsilon\xi^2}\right)$ . If we consider that  $p$  to be a reasonable number (e.g., at least grater than 0.05), we can consider it a constant factor that is independent from the input's size. The asymptotic run-time is proved to be  $\tilde{O}\left(\frac{\mu\mathbf{A}k^2m}{\theta\epsilon\xi^2}\right)$ .  $\square$

## C Experiments

### C.1 Factor score ratios distribution in real data

Throughout the work, we often claim that real datasets for machine learning are low-rank and that the distribution of their singular values is so that a few of them are much bigger than the rest. To verify this fact we have selected four datasets for machine learning and investigated the distribution of the factor score ratios  $\frac{\sigma_i^2}{\sum_j \sigma_j^2}$  in all of them. The four datasets that we have selected are: MNIST, Fashion MNIST, and CIFAR-10 for image classification, and Research Paper for text classification. We briefly describe the datasets and our pre-processing steps. We show the factor score ratios' distribution in Figure 2.

**MNIST** MNIST [40] is probably the most used dataset in image classification. It is a collection of 70000 images of  $28 \times 28 = 784$  pixels. Each image is a black and white hand-written digit between 0 and 9 and it is paired with a label that specifies the digit. Since the images are black and white, they are represented as arrays of 784 values that encode the lightness of each pixel. The dataset, excluding the labels, can be encoded in a matrix of size  $70000 \times 784$ . We shift the dataset to row mean 0 and normalize it so that  $\sigma_{max} \leq 1$ .

**Fashion MNIST** Fashion MNIST [60] is a recent dataset for benchmarking in image classification. Like the MNIST, it is a collection of 70000 images composed of  $28 \times 28 = 784$  pixels. Each image represents a black and white fashion item among {T-shirt/top, Trouser, Pullover, Dress, Coat, Sandal, Shirt, Sneaker, Bag, Ankle boot}. Each image is paired with a label that specifies the item represented in the image. Since the images are black and white, they are represented as arrays of 784 values that encode the lightness of each pixel. The dataset, excluding the labels, can be encoded in a matrix of size  $70000 \times 784$ . We shift the dataset to row mean 0 and normalize it so that  $\sigma_{max} \leq 1$ .

**CIFAR-10** CIFAR-10 [38] is another widely used dataset for benchmarking image classification. It contains 60000 colored images of  $32 \times 32$  pixel, with the values for each of the 3 RGB colors. Each image represents an object among {airplane, automobile, bird, cat, deer, dog, frog, horse, ship, truck} and is paired with the appropriate label. We use all the images, reshaping them to unroll the three channels in a single vector. The resulting size of the dataset is  $60000 \times 3072$ . We shift the dataset to row mean 0 and normalize it so that  $\sigma_{max} \leq 1$ .

**Research Paper** Research Paper [24] is a dataset for text classification, available on Kaggle. It contains 2507 titles of papers together with the labels of the venue where they have been published. The labels are {WWW, INFOCOM, ISCAS, SIGGRAPH, VLDB}. We pre-process the titles to compute a contingency table of  $papers \times words$ : the value of the  $i^{th} - j^{th}$  cell is the number of times that the  $j^{th}$  word is contained in the  $i^{th}$  title. We remove the English stop-words, the words that appear in only one document, and the words that appear in more than half the documents. The result is a contingency table of size  $2507 \times 2010$ .

For all the four datasets, we compute the singular values and their factor score ratios and we plot them. The results of Figure 2 show a rapid decrease of the factor score ratios in all the datasets, confirming the expectations.

## C.2 Image classification with quantum PCA

To provide the reader with a clearer view of our new algorithms and their use in machine learning, we provide experiments on quantum PCA for image classification. We perform PCA on the three datasets for image classification (MNIST, Fashion MNIST and CIFAR 10) and classify them with a K-Nearest Neighbors. First, we simulate the extraction of the singular values and the percentage of variance explained by the principal components (top  $k$  factor score ratios' sum) using the procedure from Theorem 8. Then, we study the error of the model extraction, using Lemma 13, by introducing errors on the Frobenius norm of the representation to see how this affects the accuracy.

**Estimating the number of principal components** We shift MNIST, Fashion MNIST and CIFAR-10 to row mean 0 and divide them by their spectral norm. We simulate Theorem 8 to decide the number of principal components needed to retain 0.85 of the total variance. For each dataset, we classically compute the singular values with an exact classical algorithm and simulate the quantum state  $\frac{1}{\sqrt{\sum_j^r \sigma_j^2}} \sum_i^r \sigma_i |\sigma_i\rangle$  to emulate the measurement process of Algorithm 1. After initializing the random object with the correct probabilities, we measure it  $\frac{1}{\gamma^2} = 1000$  times and estimate the factor score ratios with a frequentist

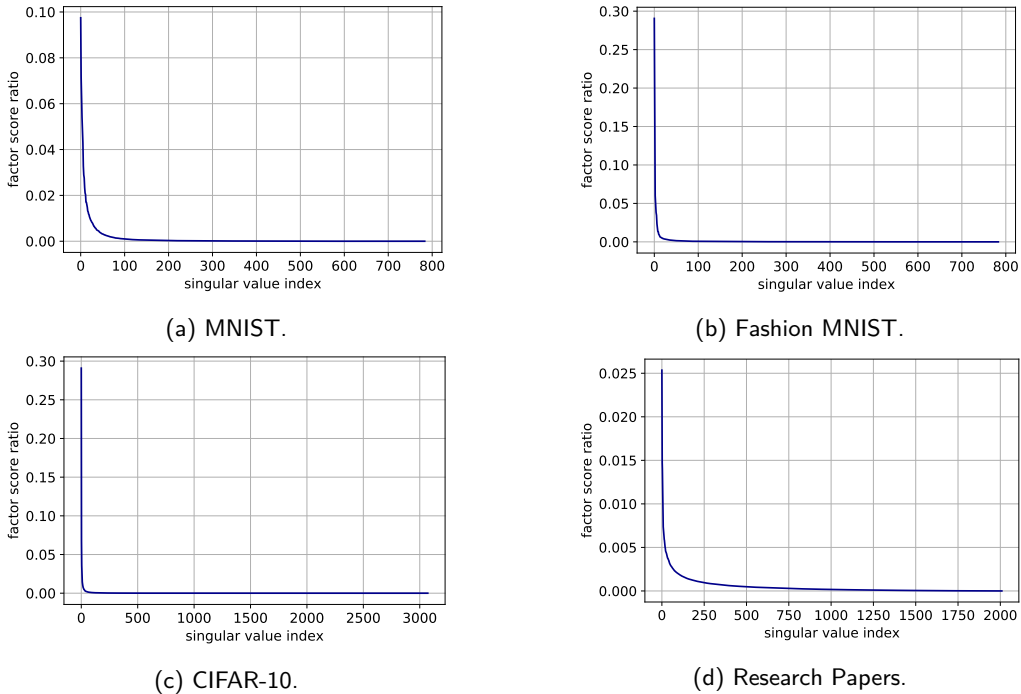


Figure 2: Factor score ratios distributions in datasets for machine learning.

Table 2: Results of the estimation of the number of principal components to retain. The parameter  $k$  is the number of components needed to retain at least  $p = 0.85$  of the total variance. The parameter  $p$  is computed with respect to the estimated  $k$ .

PARAMETER	MNIST	F-MNIST	CIFAR-10
ESTIMATED $k$	62	45	55
EXACT $k$	59	43	55
ESTIMATED $p$	0.8510	0.8510	0.8510
EXACT $p$	0.8580	0.8543	0.8514
$\gamma$	0.0316	0.0316	0.0316

approach (i.e., dividing the number of measurements of each outcome by the total number of measurements). Measuring 1000 times guarantees us an error of at most  $\gamma = 0.03$  on each factor score ratios. To determine the number of principal components to retain, we sum the factor score ratios until the percentage of explained variance becomes greater than 0.85. We report the results of this experiments in Table 2. We obtain good results for all the datasets, estimating no more than 3 extra principal components than needed. The number of principal components can be further refined using Theorem 9. When we increase the percentage of variance to retain, the factor score ratios become smaller and the estimation worsens. When the factor score ratios become too small to perform efficient sampling, it is possible to establish the threshold  $\theta$  for the smaller singular value to retain using Theorems 9 and 10. If one is interested in refining the exact number  $k$  of principal components, rather than  $\theta$ , it is possible to obtain it using a combination of the algorithms from Theorems 9, 10 and the quantum counting algorithm [4] in time that scales with the square root of  $k$ . Once that the number of principal components has been set, the next step is to use Theorem 11 to extract the top singular vectors. To do so, we can retrieve

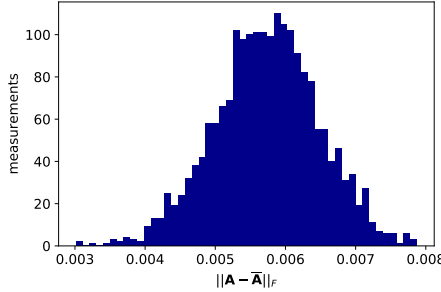


Figure 3: Introducing some error in the Frobenius norm of a matrix  $\mathbf{A}$ . The error was introduced such that  $\|\mathbf{A} - \bar{\mathbf{A}}\| \leq 0.01$ . The figure shows the distribution of the error over 2000 measurements.

the threshold  $\theta$  from the previous step by checking the gap between the last singular value to retain and the first to exclude.

**Studying the error in the data representation** We continue the experiment by checking how much error in the data representation a classifier can tolerate. We compute the exact PCA's representation for the three datasets and perform 10-fold Cross-validation error using a k-Nearest Neighbors with 7 neighbors. For each dataset we introduce error in the representation and check how the accuracy decreases. To simulate the error, we perturb the exact representation by adding truncated Gaussian error (zero mean and unit variance, truncated on the interval  $[-\frac{\xi}{\sqrt{nm}}, \frac{\xi}{\sqrt{nm}}]$ ) to each component of the matrix. The graph in Figure 3 shows the distribution of the effective error on 2000 approximation of a matrix  $\mathbf{A}$ , such that  $\|\mathbf{A} - \bar{\mathbf{A}}\| \leq 0.1$ . The distribution is still Gaussian, centered almost at the half of the bound. The results show a reasonable tolerance of the errors, we report them in two sets of figures. Figure 4 shows the drop of accuracy in classification as the error bound increases. Figure 5 shows the trend of the accuracy against the effective error of the approximation.

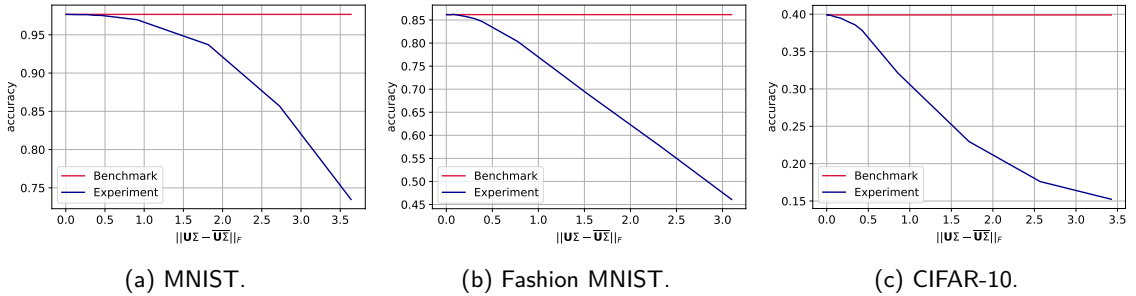


Figure 4: Classification accuracy of 7-Nearest Neighbor on three machine learning datasets after PCA's dimensionality reduction. The drop in accuracy is plotted with respect to the *bound* on the Frobenius norm of the difference between the exact data representation and its approximation.

**Analyzing the run-time parameters** As discussed in Section 4, the model extraction's run-time is  $\tilde{O}\left(\left(\frac{1}{\gamma^2} + \frac{kz}{\theta\sqrt{p}\delta^2}\right)\frac{\mu(\mathbf{A})}{\epsilon}\right)$ , where  $\mathbf{A} \in \mathbb{R}^{n \times m}$  is PCA's input matrix,  $\mu(\mathbf{A})$  is a parameter bounded by  $\min(\|\mathbf{A}\|_F, \|\mathbf{A}\|_\infty)$ ,  $k$  is the number of principal components retained,  $\theta$  is the value of the last singular value retained,  $\gamma$  is the precision to estimate the factor score ratios,  $\epsilon$  bounds the absolute error on the estimation of the singular values,  $\delta$  bounds the  $\ell_2$  norm of the distance between the singular vectors and their approximation,

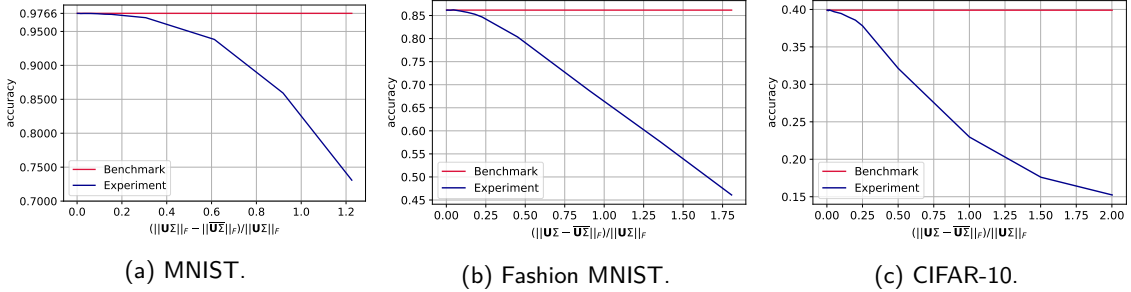


Figure 5: Classification accuracy of 7-Nearest Neighbor on three machine learning datasets after PCA's dimensionality reduction. The drop in accuracy is plotted with respect to the effective Frobenius norm of the difference between the exact data representation and its approximation.

and  $z$  is either  $n, m$  depending on whether we extract the left singular vectors, to compute the classical representation, or the right ones, to retrieve the model and allow for further quantum/classical computation. This run-time can be further lowered using Theorem 10 if we are not interested in the factor score ratios. The aim of this paragraph is to show how to determine the run-time parameters for a specific dataset. We enrich the parameters of Table 2 with the ones in Table 3 and we discuss how to compute them. From the previous paragraphs it should be clear how to determine  $k, \theta, \gamma$  and  $p$ , and it is worth noticing again that  $1/\sqrt{p} \simeq 1$ . To bound  $\mu(\mathbf{A})$  we have computed  $\|\mathbf{A}\|_F$  and  $\|\mathbf{A}\|_\infty$ . To compute the parameter  $\epsilon$  we have considered two situations: we need to allow for a correct ordering of the singular values; we need to allow for a correct thresholding. We refer to the first as the ordering  $\epsilon$  and to the second as the thresholding  $\epsilon$ . To compute the first one it is sufficient to check the smallest gap between the first  $k$  singular values of the dataset. For the last one, one should check the difference between the last retained singular value and the first that is excluded. It follows that the thresholding  $\epsilon$  is always smaller than the ordering  $\epsilon$ . For sake of completeness, we have run experiments to check how the Coupon Collector's problem changes as  $\epsilon$  increases. Recall that in the proof of Theorem 11 we use that  $\frac{1}{\sqrt{\sum_i^k \frac{\sigma_i^2}{\bar{\sigma}_i^2}}} \sum_i^k \frac{\sigma_i}{\bar{\sigma}_i} |\mathbf{u}_i\rangle |\mathbf{v}_i\rangle |\bar{\sigma}_i\rangle \sim \frac{1}{\sqrt{k}} \sum_i^k |\mathbf{u}_i\rangle |\mathbf{v}_i\rangle |\bar{\sigma}_i\rangle$  to say that the

number of measurements needed to observe all the singular values is  $O(k \log(k))$ , and this is true only if  $\epsilon$  is small enough to let the singular values distribute uniformly. We observe that the thresholding  $\epsilon$  always satisfy the Coupon Collector's scaling, and we have plotted the results of our tests in Figure 6. Furthermore, we have computed  $\delta$  by using the fact

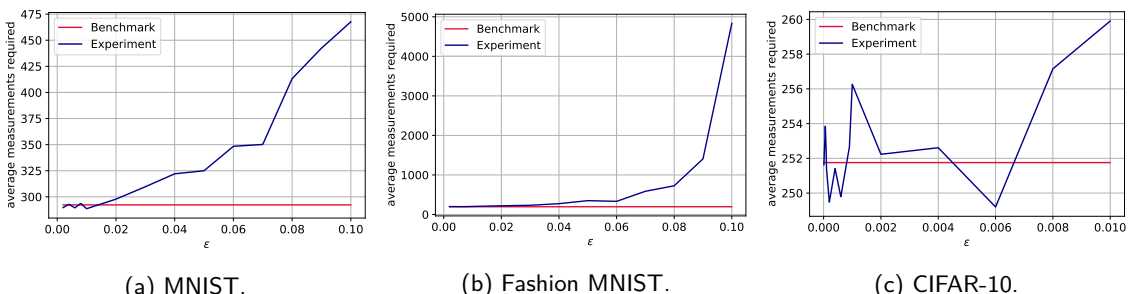


Figure 6: Number of measurements required to obtain all the  $k$  singular values from the quantum state  $\frac{1}{\sqrt{\sum_i^k \frac{\sigma_i^2}{\bar{\sigma}_i^2}}} \sum_i^k \frac{\sigma_i}{\bar{\sigma}_i} |\bar{\sigma}_i\rangle$ , where  $\|\sigma_i - \bar{\sigma}_i\| \leq \epsilon$ , as  $\epsilon$  increases. The benchmark line is  $k \log_{2.4}(k)$ .

that  $\|\mathbf{A} - \bar{\mathbf{A}}\| \leq \sqrt{k}(\epsilon + \delta)$  (Lemma 13). By inverting the equation and considering the

Table 3: Run-time parameters.

PARAMETER	MNIST	F-MNIST	CIFAR-10
ORDR. $\epsilon$	0.0003	0.0003	0.0002
THRS. $\epsilon$	0.0030	0.0009	0.0006
$\ \mathbf{A}\ _F$	3.2032	1.8551	1.8540
$\ \mathbf{A}\ _\infty$	0.3730	0.3207	0.8710
$\theta$	0.1564	0.0776	0.0746
$\delta$	0.1124	0.0106	0.0340

thresholding  $\epsilon$  we have computed an estimate for  $\delta$ . In particular, we have fixed  $\|\mathbf{A} - \bar{\mathbf{A}}\|$  to the biggest value in our experiments so that the accuracy doesn't drop more than 1%. Since we have considered the values of the effective errors instead of the bounds, our estimates are pessimistic. These results show that Theorem 8, 9 and 10 can already provide speed-ups on datasets as small as the MNIST. Even though their speed-up is not exponential, they still run sub-linearly on the number of elements of the matrix even though all the elements are taken into account during the computation, offering a polynomial speed-up with respect to their traditional classical counterparts. On the other hand, Theorem 11 requires bigger datasets. On big low-rank datasets that maintain a good distribution of singular values, these algorithms are expected to show their full speed-up. As a final remark, the parameters have similar orders of magnitude.